1969

An experimental investigation of a water heat pipe

Nathan Kalowski
Lehigh University

AN EXPERIMENTAL INVESTIGATION OF A WATER HEAT PIPE

by

Nathan Kalowski

A THESIS

Presented to the Graduate Committee

of Lehigh University

in Candidacy for the Degree of

Master of Science

in

The Department of Mechanical Engineering and Mechanics

Lehigh University

1969

This thesis is accepted and approved in partial fulfillment of the requirements for the degree of Master of Science.

April 7, 1969
(date)

Edward K. Levy
Professor in charge

Ferdinand P. Meer
Chairman of Department

ACKNOWLEDGMENT

I wish to thank Dr. Edward K. Levy for the initiation of this project and for his unending patience. I would also like to thank Professor Thomas Jackson for his much appreciated advice and his continual interest. I especially am grateful to Frank Pehacek, our machinist, without whose assistance this project would not have been completed.

TABLE OF CONTENTS

LIST OF FIGURES

ABSTRACT

A stainless steel water heat pipe instrumented with external surface thermocouples, internal thermocouples and pressure gages was designed, built, and operated.

The operating condition of the heat pipe was controlled by manipulation of a resistance heater in the evaporator section and an annulus type water cooling jacket in the condenser section.

Temperature profiles were obtained and a "temperature dip" effect noted at lower operating heat fluxes and large cooling water-vapor temperature gradients, i.e., (T_v-T_f). The effect was attributed to non-uniform condensation. Pressure measurements seemed to substantiate the saturated liquid-vapor model.

At higher operating ranges designated by Region I, as opposed to Region II, where there was a "dip" effect, the vapor temperature was isothermal.

Thermal conductivity calculations showed the condenser wick conductivity increasing with increasing power levels and operating temperature while the evaporator wick conductivity decreasing with increasing power levels and operating temperature. Values of thermal conductivity were found to vary from .5 BTU/Hr. Ft.^{o}F To 5 BTU/Hr. Ft.^{o}F depending on the power input and operating temperature.

I. INTRODUCTION

(1.) A Brief Description of the Heat Pipe Device

A heat pipe is a closed system, containing a working fluid, that utilizes an evaporation-condensation cycle to transport thermal energy. It is the latent heat of evaporation, the change in enthalpy between the liquid phase and the vapor phase at the same pressure and temperature, that allows the working fluid of the heat pipe to absorb and reject thermal energy and still remain isothermal.

A sealed circular pipe is the most frequent heat pipe configuration. Along the inside diameter of the pipe is a porous material. This porous structure, depending on the material, has a certain porosity i.e. void fraction. It is this void fraction that limits the amount of working fluid that is introduced into the system.

The heat pipe, thus, operates in a cycle. The fluid is evaporated in one section and travels down the center passage to the condenser where it is recycled to the evaporator section once again by the porous structure called the wicking.

(2.) The Historical Development of the Heat Pipe

In 1960 D. C. Thomson (1) developed the idea of a working heat pipe device and filed a patent. George M. Grover (2) of Los Alamos Scientific Laboratory hit on the devise independently and coined the name "heat pipe". Grover was also the first to formulate the applicability

of the heat pipe. Cotter (3), also of Los Alamos, in 1964, developed the first quantitative analysis of the operation of a heat pipe. Cotter's equations assume one-dimensional, incompressible flow with suction and blowing.

Grover and Cotter are accepted as the founding fathers of the heat pipe device and almost all the recent developments into the heat pipe have been initiated by their initial work.

(3.) The Mechanics of Operation of a Heat Pipe

The most frequent heat pipe geometry is shown schematically in Fig. (1). As stated previously, the heat pipe consists of a pipe with a capillary structure attached to its inner wall. This cylindrical chamber, when evacuated, is filled with a specific amount of working fluid depending on the dimensions and porosity of the capillary structure.

The operation of a heat pipe can best be explained and visualized by a parametric pressure balance. That is, the maximum amount of energy will be transferred when

$$\left[\begin{array}{l}\text{Pumping}\\ \text{Capacity}\\ \text{of the}\\ \text{Wick}\end{array}\right] = \left[\begin{array}{l}\text{Pressure Drop}\\ \text{in the Vapor}\\ \text{Passage}\end{array}\right] + \left[\begin{array}{l}\text{Pressure Drop}\\ \text{of the Liquid}\\ \text{Return in the}\\ \text{Wick}\end{array}\right] \pm \left[\begin{array}{l}\text{(if the pipe}\\ \text{is other than}\\ \text{horizontal)}\\ \text{Gravity Effect}\end{array}\right]$$

or in equation form,

$$\Delta P_c = \Delta P_v + \Delta P_L \pm \Delta P_G \qquad \text{(I.)}$$

Where

ΔP_c = the pumping capacity of the wick

ΔP_l = total liquid static pressure drop

ΔP_v = total vapor static pressure drop

ΔP_G = the pressure drop due to gravity

These pressure drops and vapor mass flow are illustrated schematically in Fig. (2).

One portion of the pipe serves as the heat source and it is this section that is called the evaporator. Thermal energy travels down the vapor passage due to pressure gradient ΔP_v . The section in which the vapor condenses is appropriately called the condenser. The pumping action of the capillary, ΔP_c , forces the fluid into the porous structure in the condenser portion and out into the vapor passage in the evaporator section. The surface tension of the fluid draws the fluid through the capillary due to the pumping action of the wick. The flow of the fluid through the many small interconnected pores and channels of the wicking causes the pressure drop ΔP_l . If the pipe were operating other than in the horizontal position, depending on the orientation of the liquid return in the pipe, gravity would either improve or retard the recycling of the fluid through the capillary.

For the heat pipe to start and maintain a maximum thermal energy transfer, equation (1.) must hold. That is, if the combined pressure

gradients of vapor, liquid, and gravity were greater than the pumping capacity of the wick, it would be impossible to transfer any additional thermal energy. This is obvious because once the maximum pumping capacity of the wicking is reached, no matter how much additional energy is added, the wicking would not be able to pump and re-cycle the fluid at the required rate.

Figure (3) shows the theoretical pressure drops for this heat pipe if the permeability characteristic, b, is 10. ΔP_T is the combined vapor and liquid pressure drops. Again, once the ΔP_c line is intersected at a particular operating temperature; the maximum heat flux is likewise reached.

The pressure gradients were calculated using Cotter's one dimensional analysis. For this particular heat pipe, the pressure gradients were evaluated from

$$\Delta P_L = \frac{b \nu_L \breve{Q}}{A_w \rho_L h_{fg}} \qquad (2.)$$

$$\Delta P_v = \frac{(1 - 4/\pi^2)\,\dot{Q}^2}{8\,\rho_v\,\pi_v^4\,L^2} \qquad (3.)$$

$$\Delta P_c = \frac{2\sigma}{r_c} \qquad (4.)$$

where

$$\frac{1}{r_c} = \left(\frac{1}{r_1 + r_{w_1}} + \frac{1}{r_2 + r_{w_2}} \right) \qquad (5.)$$

The heat pipe coordinate and geometry configuration is shown in Fig. (4). The ΔP_L equation shown above does not include a gravity term because the heat pipe was operated in a horizontal position in this investigation.

(4.) The State of the Art

The design of a heat pipe is highly empirical due to the great number of variables that enter into the design of a pipe. Parker and Hanson (4) outline the optimization trends that should be followed in choosing a suitable working fluid. However, a great deal of information is still needed for choosing a capillary structure. Factors such as permeability characteristic and the effective porosity enter into the performance of a pipe. Their precise effects, however, have never been thoroughly investigated.

The equations used to predict heat pipe performance were developed assuming steady, incompressible fluid flow. Cotter's equations give good agreement at relatively high vapor densities. Experiments by Kemme (5) have shown a discrepancy between theory and experiment for heat pipes in operation in the low vapor pressure region with high velocity vapor and returning liquid.

Levy (6) investigated this effect and formulated a perfect gas model and a two phase model. His analysis concludes that the gas-dynamic choking phenomenon rather than the pumping capacity of the wick can be the limiting factor for maximum heat transfer in the low vapor pressure region.

Heat pipe technology is at the stage where design is highly empirical, much being unknown about the pipe, its performance and limitations until actually built and operated.

(5.) Investigation Objectives

Investigation objectives in this report were as follows:

a.) To design, build and operate a stainless-steel water heat pipe.

b.) To obtain detailed axial internal and external temperature distributions.

c.) To evaluate the effective wick conductivities for various operating conditions.

II. APPARATUS

(1.) Design Considerations

The design of a heat pipe is highly empirical. This is because of the many variables that enter into the operating conditions of the device.

The variables include the material of wick and pipe; the pipe's size and shape; the type of capillary structure; the choice of working fluid; and the evaporator-condenser length ratio.

Heat pipe materials mentioned in the literature (7) have been glass, ceramic, copper, stainless steel, nickle, and molydenum. Working fluids mentioned have included methanol, acetone, water, mercury, potassium, sodium, lithium, lead, bismuth, and a range of inorganic salts. Capillary structures include sintered porous mixtures, woven mesh screening, fiberglass, longitudinal slots, and combinations of these structures in various geometries. Heat pipes range in size from 1/4" diameter to a couple of inches in diameter; from a few inches long to several feet. The power transferred by heat pipes range from a few watts to thousands of watts.

When designing a heat pipe device it is obvious that all the variables must be taken into account. To obtain the desired operating conditions, a unit must be designed with the compatability of the materials and working fluid in mind and the temperature-heat flux range intended.

A stainless steel Dutch Twill wire cloth was chosen as the capillary structure. Distilled water was chosen as the working

fluid for various reasons. Water is a safe fluid as compared to the liquid metals.

The surface tension and latent heat of vaporization properties of water are not as good as that of the liquid metals. However, water has a relatively good vapor pressure curve for the intended operating temperature range and its availability, safeness, and purity is excellent.

Compared to other non-liquid metal working fluids such as ammonia, methenol, and acetone, distilled water has much more favorable surface tension and latent heat properties.

A stainless steel thin walled tube was chosen as the pipe container. A very fine stainless steel cloth was obtained for the capillary structure because of its compatability with water; its easiness in handling; and its high pumping capacity due to extremely small capillary pores.

The dimensions of the heat pipe were purposefully large so that few restrictions and limitations would be imposed on the instrumentation, handling, and service.

The heat pipe geometry constants are presented in Appendix A. Figure (5) shows a schematic diagram of the heat pipe experimental apparatus.

(2.) Temperature, Power, and Pressure Measurements

(a.) Temperature

Twenty-four gage Leeds & Northrup copper-constantan thermocouple wire, with silicon impregnated asbestos on each wire and glass braid

on both, were used to measure surface and vapor temperatures.

Fig. (6) shows the positions of the internal and external thermocouples. The thermocouples were fabricated with a mercury-variac bath. The external surface thermocouples were installed by soldering the head of each thermocouple into slight recesses in the surface of the pipe.

The bare wire from the bead to the glass insulation was insulated with glycol. The thermocouples in the evaporator, shown in Fig. (6), were soldered to the surface as previously described and brought out through slots in the evaporator. The evaporator jacket was machined out of a 6061 aluminum alloy rod and sliced in half. Slots were milled for the thermocouple leads and hose clamps were used to compress and hold the jacket on the pipe. Silicone grease, an excellent thermal conductive material, was applied between the outer wall of the pipe and the inner wall of the jacket to eliminate air pockets.

The soldered thermocouples in the cooling jacket were also tied down to insure their endurance through testing. The leads of these thermocouples were brought through holes in the end wall of the cooling jacket next to the adibatic section of the heat pipe.

Internal temperatures were measured by inserting a 3/16"D by 25" long stainless steel probe down the center of the vapor passage of the heat pipe.

Four copper-constantan thermocouples identical to those used for surface measurements were positioned on the probe. The beads were brought through the probe wall and soldered in place. The leads were brought out through the center of the probe. Two stainless steel 24

gage, four hole, teflon sealant, transducer glands were used to seal the bare wire brought out of each endcap. Ceramic insulators insured no contact between wires before and after the sealant. Twenty-one temperature measurements were made: fourteen surface, four internal, two cooling water, and one water bucket measurement.

The thermocouples were hooked up to two L & N rotary selector switches and the temperatures measured with a L & N millivolt potentiometer.

(b.) Power

A voltmeter and ammeter were hooked up to the resistance heating tape to measure the power generated. With the voltmeter in series and an ammeter in parallel, a variac was used to vary the power input. For resistance heating the power factor is one and, thus, the voltage-amperage product yields the power in watts. A "Brisk-heat" type heating tape provided the necessary power input. The heating tape was merely a resistance heater wrapped with braids of fiberglass cloth. This tape was 1 inch in width and 48 inches in length with a rating of 390 watts.

(c.) Pressure Measurement

A vacuum and pressure gage measured the operating pressure of the heat pipe. The vacuum gage subdivisions were .2"HG while the pressure gage was subdivided into .25 PSI increments.

The heat pipe was almost entirely operated below atmospheric conditions. Except for a few data points and occasional outgassing, the vacuum gage was used to indicate the operating pressure. Both

gages were calibrated initially against a U-tube mercury manometer.

(3.) Heat Source and Sink

The heat source consisted of a 10 inch by 2 1/2 inch diameter aluminum cylinder fitted on the pipe surface. Slots were milled in the cylinder for the thermocouple leads. A "Briskheat" 390 watt resistance heating tape was used as a power source. The cylinder diffused the non-uniformities of temperature produced by the tape.

The heat sink was a 10 inch, 2 1/4 inch O.D. brass pipe inserted over the condenser section. The ends of the annulus were fitted with "O" rings to insure a waterproof seal. The inlet cooling water mass flow was controlled by a needle valve and both the inlet and outlet tubes were located perpendicular to the brass pipe. The heat sink, source and adiabatic sections were insulated with fiberglass wool. Figure 25 describes the heat source, sink, and pipe.

III. CALIBRATION OF SYSTEM

(1.) Thermocouple Check

The validity of the temperature data depended on the accuracy of the thermocouples. Once the thermocouples were manufactured with the mercury-variac bath they were inserted into boiling water and connected to a potentiometer. The potentiometer reading was checked against a Bureau of Standards thermometer placed in the boiling water.

The thermocouples were positioned on the pipe and probe and a VTVM was used to check the thermocouple instrumentation.

Finally, once the system was assembled, the thermocouples were monitored for an isothermal condition and for various small heat fluxes. All these tests were conducted with the pipe evacuated and insulated and showed that all the thermocouples with the exception of number 6 registered properly.

(2.) Heat Loss

A calibration of the heat losses must be accounted for when the pipe is in operation. For a given heat flux input; part is carried away by the cooling water, but most is lost through the insulation. Thus, not all the heat is transferred to the working fluid.

The calibration of heat losses was determined by simulating the operation of the heat pipe. That is, heat was added while the cooling jacket was in operation. The pipe, however, was evacuated.

From the first law of thermodynamics

$$Q = \Delta U + W \qquad (6.)$$

W is zero for the system so that when the system is in equilibrium ΔU must also be zero and the heat in must be the heat lost.

A cooling water rate of 10 LBM per minute was set. Various values heat fluxes, such as 2, 4, 6, and 8 watts, were used. The cooling water inlet temperatures were varied for the fluxes to simulate approximate axial temperature gradients along the pipe and radially through the insulation. When the system reached thermal equilibrium for a given heat flux and cooling water temperature, thermocouple readings were taken along the surface of the heat pipe. Fig. (6) reveals a linear relationship between $(T_E - T_c)$ and $(T_E - T_\infty)$ at a constant heat flux. T_E is the average temperature of the evaporator; T_c the average temperature of the cooling jacket; and T_∞ is the environmental temperature. Knowing these three values, a heat loss can be determined from Fig. (7).

IV. EXPERIMENTAL RESULTS

The subdivisions of this section tabulate condensed operating data and effective wick thermal conductivities.

Section (1) tabulates data corrected for thermocouple conduction errors and heat losses in the manner it was obtained during testing. That is for a given cooling water temperature, T_f, and constant mass flow rate of 10 LBM. per minute, various values of power, Q, were put into the system.

For each cooling water temperature and various heat fluxes, data from thermocouples 1-20 and pressure gages were recorded. Thus, by controlling Q and T_f the heat pipe operating temperature, T_v, could be regulated.

T_f had values of approximately 45°F, 70°F, 90°F, 112°F, and 140°F. Power inputs ranged from 40 to 350 watts for each value of T_f. Again, Section (1) lists the surface and vapor temperatures for Region I and Region II. Section (2) tabulates effective wick thermal conductivities only for Region I and is discussed in detail in Section V. Finally, Section (3) correlates the net heat flux, Q_N, with the pressure readings, P_A, and corresponding saturation temperatures for both Region I and II. Discussion of all results are reserved for Section V.

The raw and uncorrected operating data can be found in Appendix C.

(1.) Condensed and Corrected Profile Data

		T. C. #											
Tf	Qn	2	3	4	5	7	8	9	10	11	13	15	16
°F	Watts	°F											
48.0	43.2	133.0	133.8	135.0	131.0	131.0	67.4	48.0	48.0	48.0	48.0	132.4	132.0
45.0	71.5	131.8	133.4	135.8	136.8	130.0	66.0	49.7	46.2	48.1	44.8	129.5	128.5
46.0	122.5	143.2	146.0	148.8	136.0	134.1	71.2	49.2	47.9	51.1	46.0	133.8	133.2
46.0	151.0	148.1	151.0	154.0	137.5	135.9	73.0	47.3	42.2	49.5	46.0	135.5	135.3
47.0	197.0	170.2	172.0	174.8	148.5	146.0	83.3	52.6	51.8	55.0	54.5	144.2	144.0
48.0	248.0	190.0	190.5	--	158.8	157.0	98.8	53.6	54.4	56.8	57.5	154.2	154.0
46.0	297.5	208.4	210.2	212.2	172.5	170.0	111.0	57.2	59.9	62.0	62.7	166.5	165.9
48.0	346.0	229.2	232.8	234.5	183.5	178.4	119.0	54.7	58.4	59.4	70.7	172.0	171.8
71.0	48.5	136.4	137.8	139.2	134.0	133.8	85.2	72.3	71.8	71.6	71.0	135.2	134.8
71.0	71.0	140.4	142.0	144.0	137.0	136.40	87.2	73.9	73.9	77.1	70.8	137.5	136.8
70.0	97.0	145.8	148.4	150.0	140.4	139.8	88.5	70.8	70.8	74.5	70.0	140.0	139.5
70.0	118.0	148.5	151.7	153.5	142.4	141.8	91.0	--	--	--	--	142.0	141.8
70.0	152.8	161.9	165.0	163.0	150.5	149.4	97.2	73.2	73.8	76.4	76.6	149.5	149.2
70.0	200.5	179.0	180.8	183.2	162.8	161.5	109.0	74.8	75.6	77.7	78.3	160.0	158.0

(1.) Condensed and Corrected Profile Data

T. C. #	
17	18
52.0	113.8
49.8	124.0
114.0	132.8
125.5	134.5
141.0	144.0
154.1	154.2
165.9	166.0
171.9	172.0
75.8	130.4
87.8	133.2
128.2	138.4
136.0	141.0
147.2	148.5
158.0	158.0

(1.) Condensed and Corrected Profile Data

		T. C. #											
T_f	Q_n	2	3	4	5	7	8	9	10	11	13	15	16
°F	Watts	°F											
70.0	243.5	203.5	201.8	201.5	173.8	171.5	120.8	78.0	79.9	81.5	83.3	169.9	169.5
70.0	295.0	218.5	216.4	220.2	181.0	178.4	127.0	76.4	79.6	80.2	87.3	176.0	175.5
70.0	352.0	239.8	239.4	240.0	191.5	189.2	136.8	76.4	78.4	80.4	89.2	184.8	183.2
87.9	55.5	139.0	141.8	142.8	135.9	134.0	101.0	88.8	91.7	88.8	98.7	134.0	133.9
86.7	78.5	131.3	132.2	134.0	129.0	128.0	98.5	89.3	89.3	92.1	89.3	128.0	127.5
88.0	115.0	148.5	152.3	156.0	144.3	142.2	106.4	91.2	91.2	92.0	93.8	142.1	142.0
88.5	139.5	162.0	167.5	160.0	154.5	152.0	112.0	93.3	93.8	142.1	95.7	151.5	151.0
88.3	190.0	182.0	183.8	176.0	164.1	162.1	123.0	93.0	94.3	94.3	99.4	162.0	162.0
93.0	248.5	220.8	212.1	215.2	182.5	234.8	141.8	96.2	97.8	99.1	106.1	179.8	179.0
92.0	296.0	239.2	228.4	230.0	191.5	189.8	149.5	98.1	100.3	102.2	110.4	186.1	179.9
92.0	342.0	257.8	248.0	253.2	199.0	197.0	153.9	98.4	102.4	100.0	110.9	190.3	190.0
112.0	42.3	146.0	145.5	146.8	143.2	143.5	119.8	--	--	--	--	144.2	143.5
112.0	70.0	150.0	151.0	152.1	146.0	146.1	120.8	112.6	112.8	114.9	113.3	146.8	146.0
113.0	129.5	172.4	174.8	175.1	165.8	165.8	133.5	115.9	117.0	117.8	119.1	166.4	165.2

(1.) Condensed and Corrected Profile Data

T. C. #	
17	18
169.5	169.8
175.5	175.8
182.4	182.5
131.0	133.9
122.0	126.2
141.8	142.0
151.2	151.2
162.0	162.0
179.0	179.9
186.0	186.0
190.1	190.1
118.5	141.8
145.0	146.2
165.5	166.0

(1.) Condensed and Corrected Profile Data

		T. C. #											
T_f	Q_n	2	3	4	5	7	8	9	10	11	13	15	16
°F	Watts	°F											
114.0	150.0	181.2	184.4	186.2	172.4	172.0	140.2	118.8	120.4	121.7	124.3	172.4	171.9
112.0	198.0	215.1	205.0	--	181.2	180.0	150.8	116.0	118.4	120.2	125.6	180.0	179.0
114.0	246.0	234.2	222.4	227.9	189.9	189.0	158.8	114.6	116.4	120.7	127.6	186.5	186.0
114.0	316.5	262.0	246.8	253.0	204.0	202.4	169.0	120.2	121.0	126.8	130.2	197.8	197.0
115.0	337.5	268.2	253.5	259.0	208.8	205.5	170.1	--	--	--	--	206.8	202.5
140.0	70.7	169.8	170.2	172.0	165.4	165.0	153.8	145.0	145.5	145.5	145.5	166.0	165.5
139.0	121.0	198.5	192.0	186.0	178.1	177.9	160.8	144.4	145.7	146.8	149.2	178.0	177.2
141.0	138.5	209.0	200.0	195.2	181.8	181.0	164.5	147.9	148.3	148.7	149.7	181.8	180.8
140.9	185.0	226.5	216.5	216.5	191.0	190.0	170.2	145.8	146.2	148.9	149.9	189.5	188.5
140.6	243.0	244.0	235.0	239.0	203.8	201.9	179.8	147.6	149.2	152.5	155.5	200.2	200.0
140.7	283.0	255.2	239.5	252.5	210.0	209.5	186.0	147.9	149.2	152.4	155.4	207.8	207.2
139.8	344.0	272.1	255.4	264.0	219.0	218.1	192.4	146.8	148.9	153.1	156.1	215.8	215.0

(1.) Condensed and Corrected Profile Data

T. C. #	
17	18
171.9	172.0
179.2	179.5
186.1	186.2
197.0	197.5
201.5	201.6
165.5	165.8
177.2	177.8
180.8	181.0
188.8	189.0
200.0	200.1
207.2	207.3
215.0	215.5

(2.) Effective Wick Thermal Conductivity Results

Region I:

T_f	Q_N	KE		BTU/HR. FT. °F KC		KC	
°F	Watts	Max	Min	Max	Min	h=75	h=00
45	151	2.80	1.91	.416	.399	.555	.402
	197	1.77	1.51	.518	.500	.7130	.479
	248	1.265	1.250	.600	.576	.880	.547
	297.5	1.670	1.520	.673	.641	.993	.590
	346	1.420	1.295	.800	.695	1.20	.660
70	156.2	2.94	2.36	.506	.484	.685	.466
	200.5	2.48	2.02	.590	.565	.822	.528
	243.5	1.80	1.695	.655	.619	.950	.576
	295.0	1.32	1.28	.780	.680	1.115	.658
	352.0	1.50	1.490	.880	.775	1.465	.732
90	78.5	3.68	2.07	.440	.402	.611	.430
	115	4.20	1.93	.560	.530	.834	.530
	139.5	3.10	2.04	.585	.560	.875	.545
	190.0	2.22	2.02	.710	.645	1.13	.635
	248.5	1.65	1.42	.785	.692	1.22	.665
	296	1.63	1.30	.920	.790	1.50	.740
	342	1.67	1.18	1.02	.870	1.87	.820

T	QN	KE		KC		KC	
°F	Watts	Max	Min	Max	Min	h=75	h=00
112	74.5	5.10	3.08	.502	.482	.742	.492
	129.5	5.04	3.48	.645	.603	.962	.580
	150.0	4.00	2.54	.735	.660	1.03	.602
	198	1.85	1.320	.862	.730	1.37	.708
	246	1.595	1.380	.977	.802	1.785	.804
	316.5	1.535	1.15	1.10	.960	2.32	.896
140	70.7	2.76	2.13	.81	.79	.785	.646
	121	3.54	1.38	1.20	.984	1.175	.766
	138.5	2.43	1.19	1.01	.972	1.60	.795
	185	1.60	1.18	1.09	.99	1.74	.900
	243	1.45	1.29	1.28	1.09	2.32	1.00
	283	2.10	1.40	1.27	1.11	2.89	1.01
	344	2.03	1.41	1.35	1.16	3.24	1.095

(3.) Condensed Operating Data

T_f °F	Q Watts	QL	QN	PA "HG	T_{SAT} °F
48	47.2	4	43.2	4.62	130.8
45	75.5	4	71.5	4.95	133.5
46	127	4.5	122.5	5.75	139.0
46	157	6	151	6.05	141.0
47	206	9	197	6.70	145.0
48	259	11	248	8.3	154
46	310	12.5	297.5	10.55	163.5
48	361	15.0	346	12.44	171.0
71	52.5	4	48.5	5.0	133.5
71	76.5	5.5	71.0	5.3	136.0
70	103.0	6.	97	5.6	138.0
70	124.0	6	118	7.025	147.0
70	165	8.8	156.2	8.125	152.8
70	211	10.5	200.5	9.65	160.0
70	255	11.5	243.5	11.55	167.5
70	308	13	295	13.55	174.5
70	366	14	352	15.37	180.0

(3.) Condensed Operating Data

T_f °F	Q Watts	QL	QN	PA "HG	T_{SAT} °F
48	47.2	4	43.2	4.62	130.8
45	75.5	4	71.5	4.95	133.5
46	127	4.5	122.5	5.75	139.0
46	157	6	151	6.05	141.0
47	206	9	197	6.70	145.0
48	259	11	248	8.3	154
46	310	12.5	297.5	10.55	163.5
48	361	15.0	346	12.44	171.0
71	52.5	4	48.5	5.0	133.5
71	76.5	5.5	71.0	5.3	136.0
70	103.0	6.	97	5.6	138.0
70	124.0	6	118	7.025	147.0
70	165	8.8	156.2	8.125	152.8
70	211	10.5	200.5	9.65	160.0
70	255	11.5	243.5	11.55	167.5
70	308	13	295	13.55	174.5
70	366	14	352	15.37	180.0

T_f	Q	QL	QN	PA	T_{SAT}
°F	Watts			"HG	°F
86.7	59.5	4.0	55.5	4.82	132.5
87.9	82.5	4.0	78.5	5.32	136.5
88.0	120	5.0	115.0	6.32	143.0
88.5	145	5.5	139.5	7.47	149.5
88.25	198.5	8.5	190.0	9.97	161.5
90.0	269	12.5	248.5	15.115	179.5
91.5	309	13.0	296.0	17.215	185.5
91.8	357	15.0	342.0	19.015	190.0
109	74.5	4.5	70.0	6.91	146.5
111	135.0	5.5	129.5	11.06	165.80
113	159.0	9.0	150.0	12.56	171.00
110.8	210.0	12.0	198.0	15.325	180.00
112.4	259.0	13.0	246.0	17.525	185.00
112.8	331.5	15.0	316.5	22.075	196.70
114	353.0	15.5	337.5	23.95	201.0

Tf	Q	QL	QN	PA	T_{SAT}
^{o}F	Watts			"HG	^{o}F
141.2	44.2	5.0	39.20	9.59	159.5
140.0	76.7	6.0	70.7	10.55	163.7
138.9	131.0	10.0	121.0	14.45	177.50
141.0	149.0	10.5	138.5	15.55	180.70
141.4	197.0	12.0	185.0	18.60	186.5
140.7	256.0	13.0	243	22.90	198.50
140.7	297.6	14.0	283	26.90	206.5

V. DISCUSSION OF RESULTS

A summary of the data and working regimes is shown in Fig. (8), where the variation of evaporator heat flux with vapor temperature for various values of cooling water is shown.

In Region I the heat pipe functions normally. That is it is isothermal throughout the vapor passage. In Region II the vapor passage experiences a large temperature gradient between the second thermocouple (T.C. #16) in the evaporator and the first thermocouple (T.C. #17) in the condenser. Figures 9, 10, 11 show a few typical temperature profiles in Region I. Fig. (12) shows a typical temperature profile in Region II.

The phenomena of Region II occurred at low heat fluxes and large temperature gradients between the vapor temperature and the cooling water. Because of low heat fluxes and large temperature gradients, it is felt that the vapor condensed in the first portion of the condenser and that this "temperature dip" phenomenon was caused by uneven condensation of the vapor. That is most of the condensation, if not all, occurred in the initial portion of the condenser so that a severe drop in temperature was observed between $.6 < x/L < .8$ as shown in Figure 12. A sudden rise then occurred at $.8 < x/L < 1.0$ This rise in temperature might be attributed to the water present in the pressure gage line tubing. The plastic tubing was connected to the endcap of the condenser by a stainless steel 1/8 inch swagelock fitting (See Figure 25) and was observed to be filled with fluid during operation in Region I. However, during operation of the heat pipe in

Region II, fluid tended to leave the tubing and it is thought to have flowed back to the endcap. This could account for the high vapor temperature shown at $x/L = .8$ in Figure 12. It also suggests that the fluid at the downstream end of the condenser and the pressure lines had not reached equilibrium when the data was recorded.

It was necessary to verify the thermocouple probe data so as to eliminate faulty instrumentation as a reason for the "dip" effect seen in Region II.

The system was taken apart and the probe reversed. The pipe was evacuated and refilled with the same quantity of working fluid as previously recorded. The previous data was duplicated and this substantiated the validity of the internal probe.

Pressure measurement data proved the working fluid to be operating as a saturated liquid-vapor model. That is, for every vapor temperature recorded, there existed a unique operating pressure according to the clausius-clapeyron relation. This is shown in the data and from Figs. 9, 10, 11 in Region I and Fig. (12) in Region II. T_{Sat} as shown in the mentioned figures and in the data of IV-3 is the saturation temperature corresponding to the operating pressure P_A. T_{Sat} was obtained from steam tables once P_A was measured. The agreement between T_{Sat} and T_v is excellent.

The surface temperatures recorded in the evaporator and condenser were not exactly uniform and can be explained by the method of heat addition and rejection. Since a heating tape was wrapped around an aluminum collar in the evaporator section (See Fig. 25), an inherent

non-uniformity of heat was distributed according to the wrap of the tape.

The temperature non-uniformity monitored in the cooling jacket was due to the stratification of the cooling water as it entered and left the jacket annulus. That is, the cooling water flow pattern left portions of the condenser with "dead spots", such that these sections experienced lower coefficients of convection than the majority of the condenser annulus. These "hot" sections were measured for thermocouples number 12 and number 14, and it can be noted that T.C. number 12 and 14 were located immediately before the outlet tube of the cooling jacket indicating that the fluid leaving the jacket left a stagnant area in the vicinity of the exit tube. Thus, thermocouples number 12 and 14 were neglected due to an existing hot spot in that area. This hot spot was estimated to cover approximately 15% of the cooling area and is thought to be attributed to the fluid mechanics of the cooling water as it passed through the annulus of the jacket.

The thermocouple readings in the cooling jacket were corrected for conduction errors due to the flow of cooling water past the wires positioned on the surface. The correction of thermocouples 9, 10, 11, 13 are included in (1) of Section IV. A sample calculation of this correction is given in Appendix D.

Although the thermocouples were corrected for conduction errors, there still was a discrepancy between $(T_w-T_f)_{theoretical}$ and $(T_w-T_f)_{measured}$. The measured (T_w-T_f) was lower than it was calculated. The theoretical temperature difference was evaluated from

$$\left(T_w - T_f \right)_{THEORETICAL} = \frac{Q_n}{h} \qquad (7.)$$

The discrepancy might be due to the uncertainty in the value of the film coefficient, h.

For a mass flow rate of 10 LBM. per minute with T_f varying from 50°F to 140°F the value of h is calculated to lie somewhere between 75 and 85 B.T.U./Hr. Ft.^{2} °F. This range was calculated using the equation for Laminar flow in an annulus as outlined by Kreith (8). A value of h approximately equal to 175 B.T.U./Hr. Ft.^{2} °F is needed for agreement between $(T_w-T_f)_{measured}$ and $(T_w-T_f)_{theoretical}$.

It is thought that an h value this high is realistic if one considers the type of flow occurring in the cooling jacket. That is the flow does not develop uniformily in the jacket but is brought in abruptly and also brought out in the same manner. There are many thermocouple wires in the annulus causing secondary flows. The combination of the manner in which the fluid enters and leaves coupled with the induced mixing of the wires seem to indicate that h was actually of this magnitude.

(2.) Wick Thermal Conductivity

The determination of the effective thermal conductivity of wicking was a main objective in this investigation. The voids of the wicking being filled with working fluid, the question arose to the value of the wick conductivity and how the conductivity changed with various parameters.

The effective conductivity was studied for Region I only, since it was felt that the uneven condensation occurring in Region II made Region II conductivities impossible to determine from the measurements which were obtained.

Effective conductivities for both the evaporator and condenser sections were calculated. Figures (13) to (17) show the conductivities in the condenser region for various cooling jacket temperatures. Figures (18) to (22) also show wick conductivities for the evaporator region.

The scatter band of the evaporator conductivity is obtained by calculating the conductivity from the high and low temperature in the evaporator jacket and using the relation

$$K_E = \frac{Q \ln (r_i/r_v)}{2\pi L (T_v - T_w)_{MEASURED}} \qquad (8.)$$

The large variation in the conductivity as shown in Figures (18) to (22) are a result of the small temperature difference caused between the vapor temperature and the evaporator surface temperature. This can be seen from the temperature profile data and is obvious once the equation for heat conduction in a composite cylinder is studied. The scatter band decreases with increasing heat flux because the temperature difference effect is less significant as seen in the temperature profile data.

The condenser scatter envelope were two lines whose effective conductivity was calculated for surface convective coefficients of

75 (the calculated value of h based on laminar uniform flow in an annulus) and ∞ . These two lines were evaluated from

$$\frac{T_v - T_f}{Q} = \frac{\ln\left(\frac{r_i}{r_v}\right)}{2\pi K_c L} + \frac{\ln\left(\frac{r_o}{r_i}\right)}{2\pi K_{ss} L} + \frac{1}{h A_s} \qquad (9.)$$

The X's plotted on the same graphs shown in Figures (13) to (17) was found with equation (8). That is a maximum and minimum surface temperature, corrected for conduction errors as in Appendix D, was substituted into the equation to arrive at K_c as indicated by X's.

An h value of 175 B.T.U./Hr. Ft. ^{o}F represented on Figures (13) to (17) is shown extremely close to the h=175 line and the X line. From the previous discussion of the flow pattern in the annulus and the required h value to correlate $(T_w-T_f)_{theoretical}$ with $(T_w-T_f)_{measured}$ it seems likely that the X's represent the best agreement of the actual effective conductivities.

The results of the effective wick conductivity in the evaporator seem much too scattered to predict trends based both on the condenser temperature and heat flux. All that can be said is that K_e lies between 5 and 1 decreasing with increasing value of heat flux.

The effective wick conductivity of the condenser is much less scattered and its band defines a definite trend. The value of K_c increases with increasing heat flux and increasing cooling water temperature. The value of K_c lies between .4 and 4 for the lines h= ∞, 75 and between .4 and 1.2 for the X's.

Gorring and Churchill (9) presented two limiting cases for heat conduction in a porous medium. The lower limit assumes two phases conducting in series while the upper limit assumes the effective heat conductivity would occur if both phase conducted heat in parallel.

The limiting values of effective conductivity for the water-wick combination was calculated to be .510 and 3.65 B.T.U./Hr. Ft.^{o}F. Figures 13-22 show the effective conductivities and the limiting bands. The experimental values of conductivity are in excellent agreement with Gorring and Churchill's prediction.

VI. CONCLUSION

The heat pipe as a thermal energy transfer device is capable of transferring energy much more effectively than any thermally conductive material known.

In Region I the entire condenser length was utilized and calculations from the obtained data yielded heat pipe conductivities of 500 to 1000 B.T.U./Hr. Ft. ^{o}F, depending on the power level and cooling jacket water temperature.

At low power levels and operating temperatures as shown in Figure (8) a phenomenon occurred that seemed to indicate that the entire heat pipe condenser was not being utilized. Figure (12) shows a typical non-isothermal vapor temperature profile that occurred at the low levels indicating non-use of the entire condenser due to large cooling water-vapor temperature gradients and low vapor mass flows. In Region I the vapor temperature was nearly isothermal in all cases and agreed with the saturation temperatures obtained from the pressure data.

The effective wick conductivity was calculated for both the condenser and the evaporator sections. Limiting values of .5 and 3.65 B.T.U./Hr. Ft. ^{o}F were obtained from Gorring and Churchill and almost all the conductivities did fall between the two limits.

The trends of the wick conductivities did indicate a dependence on the power level and operating temperature. It is felt that the condenser wick conductivity can be narrowed to the range of .4 to 1.2 B.T.U/Hr. Ft. ^{o}F. This was discussed in Section V-2.

A permeability experiment was devised and a value of 42 obtained (See Appendix F). This value could not be used because it represented a completely compressed wick that was not representative of the wick in the heat pipe. Attempts at duplicating the heat pipe wicking for permeability measurement were unsuccessful.

The phenomenon "burn out", drying of the wick, was not observed. The "burn out" phenomenon probably did not occur due to the low operating power levels used.

The main objectives of investigation were:

1. To design, build, and operate a water heat pipe.
2. To obtain internal and external temperature data.
3. To obtain effective conductivities of the water-wick material.

These objectives were all accomplished and it can be summarized that:

1. The heat pipe did indeed function properly, yielding extremely high thermal conductivities between 500 and 1000 B.T.U./Hr. Ft. ^{o}F.
2. External and internal temperature profiles were obtained, showing, in Region I, a nearly isothermal situation as had been expected.
3. Effective wick conductivities between .5 and 5 B.T.U./Hr. Ft. ^{o}F were obtained and agreed quite well with theoretical predictions.

VII. RECOMMENDATIONS FOR FUTURE WORK

From studying the profile and conductivity results, it is obvious that more thermocouple instrumentation is needed to study the performance of the heat pipe.

Non-uniformities in the evaporator and condenser could be avoided by modifying the heating and cooling system. An induction heater instead of resistance heater would improve the data in the heat source region while a cooling jacket with inlet and outlet manifolds would result in a less stratified fluid flow.

A closed cycle cooling system utilizing a heater and cooler with a fluid other than water could tremendously improve the operating limitations of the heat pipe.

From the data it is worthwhile to note that in Region II the entire condenser section was not used and that a variable length cooling jacket with an increase in the number of internal thermocouple probes would provide information into the phenomena occurring in Region II.

Of course, investigation into the value of the permeability characteristic is needed; especially for the wound wire cloth capillary structure, where the "looseness" is the significant factor.

Investigation into the performance characteristics could be carried on by using various other non-metal working fluids as ethanol, glycerin, ammonia, and others. Different capillary structures could be inserted to determine their effects on the heat pipe performance. Finally,

the heat pipe could be operated in various positions for investigation purposes.

It is obvious that there are many variables that govern the heat pipe performance and that there is a great amount of investigation required to provide design criteria needed to predict the performance and limitations of a heat pipe.

APPENDIX A

HEAT PIPE CONSTANTS

Pipe Material:	304 stainless steel
Pipe Length:	24 inches
Pipe O.D.:	1.31 inches
Pipe I.D.:	1.17 inches
Screen Material:	Stainless steel
Screen Thickness: (per layer)	.011"
Screen Mesh:	120 x 400
Effective Pore Radius:	$.88 \times 10^{-6}$ inches
Vapor Passage Diameter:	.8150 inches
Probe Diameter:	.1875 inches
Vapor Passage Hydraulic Diameter:	.6275 inches
Evaporator Length:	10 inches
Condenser Length:	10 inches
Adiabatic Length:	2 inches
Heating Collar Diameter:	2 1/2 inches
Cooling Jacket Diameter:	2 1/4 inches O.D.
Effective Heat Pipe Length:	1 ft.
Porosity:	.658
Permeability Characteristic:	--------?

APPENDIX B

NOMENCLATURE

A	Cross-sectional area of wick
b	Dimensionless; permeability characteristic
ε	Dimensionless; porosity
h_{fg}	B.T.U./#m ; latent heat of evaporization
I	Amps; current
K_e	B.T.U./Hr. FT^{o}F; effective wick thermal conductivity in evaporator section
K_c	B.T.U./Hr. FT^{o}F; effective wick thermal conductivity in condenser section.
$\dot{M}$	#M/min; cooling water mass flow
P_A	IN. HG.; absolute corrected gage pressure
P_B	IN. HG.; barometric pressure
P_G	IN. HG.; gage pressure
Q	Watts; total heat flux
Q_L	Watts; lost heat flux
Q_N	Watts; net heat flux
ν_L	ft.SQ/sec.; kinematic viscosity for water
ρ_v	#m /ft^3; density of vapor
ρ_L	#m/ft^3 ; density of liquid
r_v	Vapor passage radius
r_j	Screen pore width; j = 1, 2.....
r_i	Inside radius of pipe
r_o	Outside " " "
r_{w_i}	Screen wire pore radius
r_c	Effective pore radius
σ	Surface tension

T_f: ^oF; cooling water temperature

T_R, T_∞: ^oF; room temperature (Environment)

T_{SAT}: ^oF; saturation temperature at operating pressure

T_v: ^oF; vapor temperature

T_w: ^oF; wall temperature

V: Volts

APPENDIX C

UNCORRECTED PERFORMANCE DATA

T. C. #	Millivolts Q = 47.2 WATTS	^{o}F		
1	2.28	132.1	I:	1.35 AMPS.
2	2.30	133.0	V:	35 VOLTS
3	2.315	133.8	T_f:	48°F
4	2.345	135.0	P_G:	25.1 IN. HG.
5	2.245	131.0	$\dot{M}$:	10.0 #m/min.
6	out	----	P_B:	29.72 IN. HG.
7	2.245	131.0	T_R:	78 °F
8	.772	67.4		
9	.370	48.8		
10	.350	48.0		
11	.350	48.0		
12	.342	47.8		
13	.350	48.0		
14	.365	48.8		
15	2.278	132.4		
16	2.266	132.0		
17	.441	52.0		
18	1.835	113.8		
19	.355	48.4		
20	.370	49.0		

UNCORRECTED PERFORMANCE DATA

T. C. #	Millivolts Q = 75.5	°F	
1	2.265	131.8	I: 1.57
2	2.310	133.4	V: 48,0
3	2.360	135.8	T_f: 45°F
4	2.390	136.8	P_G: 26.10
5	2.226	130.0	M: 10.0
6	out	----	P_B: 29.95 "HG
7	2.20	129.0	T_R: 77
8	.745	66.0	
9	.348	48.0	
10	.295	45.8	
11	.325	47.0	
12	.275	44.5	
13	.280	44.80	
14	.285	45.00	
15	2.205	129.50	
16	2.192	128.50	
17	.395	49.80	
18	2.08	124.00	
19	.275	44.50	
20	.295	45.80	

UNCORRECTED PERFORMANCE DATA

T. C. #	Millivolts Q = 127	°F	
1	2.44	139.0	I: 2.05
2	2.549	143.2	V: 62
3	2.614	146.0	T_f: 46°F
4	2.68	148.8	P_G: 25.30
5	2.37	136.0	M: 10.0
6	out	----	P_B: 29.95
7	2.325	134.10	T_R: 77
8	.855	71.20	
9	.350	48.0	
10	.335	47.2	
11	.377	49.2	
12	.77	67.0	
13	.30	46.0	
14	.330	47.2	
15	2.315	133.8	
16	2.306	133.2	
17	1.85	114.0	
18	2.29	132.8	
19	.275	44.5	
20	.305	46.0	

UNCORRECTED PERFORMANCE DATA

T. C. #	Millivolts Q = 157	°F	
1	2.525	142.1	I: 2.25
2	2.665	148.1	V: 69.8
3	2.736	151.0	T_f: 46°F
4	2.803	154.0	P_G: 25.00
5	2.405	137.5	M: 10.0
6	out	out	P_B: 29.95
7	2.365	135.9	T_R: 78.5
8	.890	73.0	
9	.327	46.8	
10	.311	46.1	
11	.361	48.2	
12	1.060	80.0	
13	.309	46.0	
14	.512	55.4	
15	2.357	135.5	
16	2.350	135.3	
17	2.115	125.5	
18	2.340	134.5	
19	.270	44.2	
20	.295	45.8	

UNCORRECTED PERFORMANCE DATA

T. C. #	Millivolts Q = 206	^{o}F		
1	2.87	161.2	I:	2.575
2	3.20	170.2	V:	80
3	3.26	172.0	T_f:	47 ^{o}F
4	3.335	174.8	P_G:	24.35
5	2.674	148.5	M:	10.0
6	out	----	P_B:	29.95
7	2.617	146.0	T_R:	77
8	1.130	83.3		
9	.405	50.5		
10	.395	50.0		
11	.440	52.0		
12	1.35	92.8		
13	.931	51.8		
14	1.166	85.0		
15	2.576	144.2		
16	2.565	144.0		
17	2.490	141.0		
18	2.564	144.0		
19	.314	46.2		
20	.345	47.8		

UNCORRECTED PERFORMANCE DATA

T. C. #	Millivolts Q = 259	^{o}F		
1	3.27	172.5	I:	2.900
2	3.715	190.0	V:	89.50
3	3.725	190.5	T_f:	48°F
4	out	----	P_G:	22.75
5	2.925	158.8	M:	10.0
6	out	----	P_B:	29.95
7	2.88	157.0	T_R:	76.0
8	1.492	98.8		
9	.425	51.5		
10	.440	52.0		
11	.465	53.5		
12	1.555	108.8		
13	.476	53.9		
14	1.47	108.0		
15	2.82	154.2		
16	2.805	154.0		
17	2.810	154.1		
18	2.815	154.2		
19	.3180	46.4		
20	.364	48.5		

UNCORRECTED PERFORMANCE DATA

T. C. #	Millivolts Q = 310	°F		
1	3.66	188.0	I:	3.15
2	4.170	208.4	V:	98.5
3	4.235	210.2	T_f:	46°F
4	4.290	212.2	P_G:	20.25
5	3.278	172.5	M:	10.0
6	out	----	P_B:	29.69
7	3.205	170.0	T_R:	80
8	1.775	111.0		
9	.460	53.0		
10	.486	54.6		
11	.524	56.0		
12	1.035	79.2		
13	.553	57.2		
14	1.620	104.2		
15	3.13	166.5		
16	3.09	165.9		
17	3.09	165.9		
18	3.095	166.0		
19	.326	46.5		
20	.381	49.2		

UNCORRECTED PERFORMANCE DATA

T. C. #	Millivolts Q = 361	°F		
1	out	----	I:	3.40
2	4.730	229.2	V:	106
3	4.830	232.8	T_f:	48°F
4	4.875	234.5	P_G:	18.35
5	3.548	183.5	M:	10.0
6	out	----	P_B:	29.69
7	3.42	178.4	T_R:	80
8	1.962	119.0		
9	.447	52.2		
10	.495	54.5		
11	.530	56.1		
12	2.165	127.9		
13	.67	62.2		
14	1.735	109.2		
15	3.255	172.0		
16	3.245	171.8		
17	3.250	171.9		
18	3.255	172.0		
19	.325	46.8		
20	.380	49.5		

UNCORRECTED PERFORMANCE DATA

T. C. #	Millivolts Q = 52.5	°F		
1	2.355	135.5	I:	1.31
2	2.381	136.4	V:	42.5
3	2.410	137.8	T_f:	71°F
4	2.449	139.2	P_G:	24.70
5	2.321	134.0	M:	10.00
6	out	----	P_B:	29.70
7	2.310	133.8	T_R:	77
8	1.172	85.2		
9	.865	71.8		
10	.850	71.0		
11	.861	71.4		
12	.852	71.0		
13	.850	71.0		
14	.870	72.0		
15	2.349	135.2		
16	2.340	134.8		
17	.955	75.8		
18	2.232	130.4		
19	.825	69.8		
20	.825	69.8		

UNCORRECTED PERFORMANCE DATA

T. C. #	Millivolts Q = 76.5	°F		
1	2.445	139.0	I:	1.56
2	2.480	140.4	V:	49
3	2.520	142.0	T_f:	71°F
4	2.560	144.0	P_G:	24.40
5	2.395	137.0	M:	10.0
6	out	----	P_B:	29.70
7	2.380	136.40	T_R:	76
8	1.220	87.2		
9	.867	72.8		
10	.867	72.8		
11	.915	74.0		
12	1.022	78.5		
13	.845	70.8		
14	.874	72.0		
15	2.405	137.5		
16	2.390	136.8		
17	1.230	87.8		
18	2.305	133.2		
19	.832	70.		
20	.832	70.		

UNCORRECTED PERFORMANCE DATA

T. C. #	Millivolts Q = 103	^{o}F		
1	2.536	142.5	I:	1.80
2	2.600	145.8	V:	57.0
3	2.670	148.4	T_f:	70°F
4	2.705	150.0	P_G:	24.10
5	2.475	140.4	M:	10.0
6	out	----	P_B:	29.70
7	2.455	139.8	T_R:	76
8	1.250	88.5		
9	.845	70.5		
10	.845	70.5		
11	.890	72.8		
12	1.580	102.5		
13	.835	70.0		
14	.980	72.4		
15	2.470	140.0		
16	2.457	139.5		
17	2.185	128.2		
18	2.430	138.4		
19	.795	68.2		
20	.810	68.8		

UNCORRECTED PERFORMANCE DATA

T. C. #	Millivolts Q = 124	°F		
1	2.600	145.5	I:	2.0
2	2.675	148.5	V:	62.0
3	2.755	151.7	T_f:	70°F
4	2.795	153.5	P_G:	23.80
5	2.530	142.4	M:	10.0
6	out	----	P_B:	29.725
7	2.505	141.8	T_R:	76
8	1.306	91.0		
9	.855	71.2		
10	.855	71.2		
11	.900	73.5		
12	1.675	106.5		
13	.857	71.2		
14	1.260	89.0		
15	2.520	142.0		
16	2.510	141.8		
17	2.370	136.0		
18	2.490	141.0		
19	.800	68.5		
20	.820	69.8		

UNCORRECTED PERFORMANCE DATA

T. C. #	Millivolts Q = 165	°F		
1	2.845	155.8	I:	2.325
2	2.990	161.9	V:	71.5
3	3.075	165.0	T_f:	70°F
4	3.022	163.0	P_G:	22.70
5	2.725	150.5	M:	10.0
6	out	----	P_B:	29.725
7	2.695	149.4	T_R:	76
8	1.500	97.2		
9	.870	72.0		
10	.882	72.4		
11	.920	74.0		
12	1.776	111.0		
13	.425	74.10		
14	1.612	104.10		
15	2.695	149.50		
16	2.687	149.20		
17	2.640	147.20		
18	2.675	148.5		
19	.805	68.8		
20	.830	70.0		

UNCORRECTED PERFORMANCE DATA

T. C. #	Millivolts Q = 211	^{o}F		
1	out	----	I:	2.61
2	3.43	179.0	V:	81
3	3.495	180.8	T_f:	70°F
4	3.530	183.2	P_G:	21.30
5	3.02	162.8	M:	10.0
6	out	----	P_B:	29.85
7	2.985	161.5	T_R:	77
8	1.730	109.0		
9	.890	73.0		
10	.900	73.5		
11	.935	74.8		
12	2.007	120.8		
13	.945	75.2		
14	1.750	110.0		
15	2.957	160.0		
16	2.940	158.0		
17	2.940	158.0		
18	2.940	158.0		
19	.80	64.0		
20	.821	69.5		

UNCORRECTED PERFORMANCE DATA

T. C. #	Millivolts Q = 255	^{o}F		
1	out	----	I:	2.870
2	4.045	203.5	V:	89.0
3	4.000	201.8	T_f:	70°F
4	3.950	201.5	P_G:	19.40
5	3.295	173.8	M:	10.0
6	out	----	P_B:	29.85
7	3.240	171.5	T_R:	80
8	2.005	120.8		
9	.940	75.0		
10	.972	76.2		
11	.99	77.2		
12	2.19	128.8		
13	1.02	78.3		
14	1.905	116.4		
15	3.192	169.9		
16	3.180	169.5		
17	3.180	169.5		
18	3.185	169.8		
19	.846	70.8		
20	.870	72.0		

UNCORRECTED PERFORMANCE DATA

T. C. #	Millivolts Q = 308	°F		
1	out	----	I:	3.15
2	4.45	218.5	V:	98
3	4.395	216.4	T_f:	70°F
4	4.490	220.2	P_G:	17.30
5	3.48	181.0	M:	10.
6	out	----	P_B:	29.75
7	3.415	178.4	T_R:	77
8	2.155	127.0		
9	.915	74.0		
10	.960	76.0		
11	.972	76.4		
12	2.262	131.8		
13	1.070	80.8		
14	2.06	123.2		
15	3.354	176.0		
16	3.340	175.5		
17	3.340	175.5		
18	3.345	175.8		
19	.805	68.8		
20	.840	70.2		

UNCORRECTED PERFORMANCE DATA

T. C. #	Millivolts Q = 366	^{o}F		
1	out	----	I:	3.42
2	5.10	239.8	V:	107
3	4.99	239.4	T_f:	70°F
4	5.115	240.0	P_G:	14.45
5	3.742	191.5	M:	10.
6	out	----	P_B:	29.72
7	3.585	189.2	T_R:	81
8	2.390	136.8		
9	.916	74.0		
10	.945	75.2		
11	.976	76.5		
12	2.065	123.5		
13	1.10	82.0		
14	2.09	124.8		
15	3.575	184.8		
16	3.535	183.2		
17	3.515	182.4		
18	3.520	182.50		
19	.809	68.4		
20	.850	71.0		

UNCORRECTED PERFORMANCE DATA

T. C. #	Millivolts Q = 82.5	°F		
1	2.400	137.2	I:	1.65
2	2.446	139.0	V:	50
3	2.505	141.8	T_f:	--
4	2.540	142.8	P_G:	25.60 "HG
5	2.365	135.9	M:	10.0
6	out	----	P_B:	29.82
7	2.326	134.0	T_R:	84
8	1.545	101.0		
9	1.270	88.8		
10	1.270	88.8		
11	1.296	90.5		
12	1.812	112.2		
13	1.276	88.8		
14	1.626	104.2		
15	2.326	134.0		
16	2.320	133.9		
17	2.245	131.0		
18	2.310	133.9		
19	1.231	87.9		
20	1.231	87.9		

UNCORRECTED PERFORMANCE DATA

T. C. #	Millivolts Q = 59.5	°F		
1	2.230	130.0	I:	1.40
2	2.255	131.3	V:	42.5
3	2.240	132.2	T_f:	--
4	2.329	134.0	P_G:	26.1
5	2.20	129.0	M:	10.0
6	out	----	P_B:	29.82
7	2.171	128.0	T_R:	84
8	1.485	98.5		
9	1.242	88.		
10	1.242	88.		
11	1.272	89.8		
12	1.702	108.		
13	1.240	88.0		
14	1.395	94.2		
15	2.175	128.0		
16	2.161	127.5		
17	2.025	122.0		
18	2.150	126.2		
19	1.206	86.5		
20	1.210	86.8		

UNCORRECTED PERFORMANCE DATA

T. C. #1	Millivolts Q = 120	°F		
1	2.634	146.5	I:	2.0
2	2.729	148.5	V:	60
3	2.817	152.3	T_f:	--
4	2.860	156.0	P_G:	24.60
5	2.580	144.3	M:	10.0
6	out	----	P_B:	29.82
7	2.531	142.2	T_R:	83
8	1.669	106.4		
9	1.285	90.0		
10	1.285	90.0		
11	1.310	90.5		
12	1.915	117.		
13	1.320	91.6		
14	1.790	111.9		
15	2.524	142.1		
16	2.515	142.0		
17	2.505	141.8		
18	2.515	142.0		
19	1.231	187.9		
20	1.237	88.0		

UNCORRECTED PERFORMANCE DATA

T. C. #1	Millivolts Q = 145	°F		
1	2.90	157.9	I:	2.175
2	3.04	162.0	V:	67.0
3	3.135	167.5	T_f:	--
4	2.956	160.0	P_G:	23.30
5	2.821	154.5	M:	10.0
6	out	----	P_B:	29.67
7	2.760	152.0	T_R:	83
8	1.795	112.0		
9	1.314	91.5		
10	1.325	91.8		
11	1.325	91.8		
12	2.027	122.0		
13	1.355	93.0		
14	1.927	117.8		
15	2.745	151.5		
16	2.735	151.0		
17	2.737	151.2		
18	2.737	151.2		
19	1.250	88.50		
20	1.250	88.50		

UNCORRECTED PERFORMANCE DATA

T. C. #	Millivolts Q = 198.5	°F		
1	3.270	172.5	I:	2.55
2	3.511	182.0	V:	78
3	3.544	183.8	T_f:	--
4	3.360	176.0	P_G:	20.80
5	3.055	164.1	M:	10.0
6	out	----	P_B:	29.67
7	3.01	162.1	T_R:	84
8	2.055	123.0		
9	1.315	91.2		
10	1.335	92.0		
11	1.335	92.0		
12	2.18	128.2		
13	1.41	95.2		
14	2.06	123.2		
15	3.991	162.0		
16	3.98	162.0		
17	3.98	162.0		
18	2.990	162.0		
19	1.245	88.0		
20	1.250	88.5		

UNCORRECTED PERFORMANCE DATA

T. C. #1	Millivolts Q = 269	^{o}F		
1	out	----	I:	2.95
2	4.506	220.80	V:	91.2
3	4.285	212.10	T_f:	93°F
4	4.365	215.20	P_G:	29.815
5	3.525	182.50	M:	10.0
6	out	----	P_B:	15.80
7	4.870	234.80	T_R:	77
8	2.505	141.80		
9	1.40	95.00		
10	1.427	96.00		
11	1.442	96.80		
12	2.557	143.80		
13	1.545	101.20		
14	2.282	154.40		
15	3.447	179.80		
16	3.436	179.00		
17	3.436	179.00		
18	3.500	179.90		
19	1.295	90.40		
20	1.312	91.00		

UNCORRECTED PERFORMANCE DATA

T. C. #	Millivolts Q = 309	°F		
1	out	----	I:	3.15
2	4.955	239.2	V:	98
3	4.710	228.4	T_f:	92°F
4	4.755	230.0	P_G:	13.70
5	3.745	191.5	M:	10.00
6	out	----	P_B:	29.815
7	3.695	189.8	T_R:	78
8	2.690	149.50		
9	1.42	95.80		
10	1.455	97.20		
11	1.481	98.40		
12	2.655	147.80		
13	1.597	103.50		
14	2.372	136.00		
15	3.612	186.10		
16	3.601	179.90		
17	3.605	186.00		
18	3.605	186.00		
19	1.307	91.00		
20	1.330	92.0		

UNCORRECTED PERFORMANCE DATA

T. C. #	Millivolts Q = 357	°F		
1	out	----	I:	3.38
2	5.490	257.8	V:	105.5
3	5.225	248.0	T_f:	92°F
4	5.367	253.2	P_G:	11.90
5	3.935	199.0	M:	10.0
6	out	----	P_B:	29.815
7	3.885	197.0	T_R:	78
8	2.800	153.9		
9	1.430	96.0		
10	1.445	97.0		
11	1.485	98.5		
12	2.495	141.3		
13	1.585	103.8		
14	2.532	142.8		
15	3.72	190.3		
16	3.705	190.0		
17	3.710	190.1		
18	3.710	190.1		
19	1.316	91.2		
20	1.340	92.4		

UNCORRECTED PERFORMANCE DATA

T. C. #	Millivolts Q = 47.25	°F		
1	2.594	145.5	I:	1.35
2	2.610	146.0	V:	35
3	2.600	145.5	T_f:	112°F
4	2.634	146.8	P_G:	23.75
5	2.548	143.2	M:	10.0
6	out	----	P_B:	29.69
7	2.550	143.5	T_R:	78
8	1.972	119.8		
9	1.835	113.8		
10	1.830	113.50		
11	1.855	114.40		
12	1.855	114.40		
13	1.806	112.40		
14	1.810	112.40		
15	2.573	144.20		
16	2.555	143.50		
17	1.950	118.50		
18	2.510	141.80		
19	1.795	112.		
20	1.757	110.5		

UNCORRECTED PERFORMANCE DATA

T. C. #	Millivolts Q = 74.5	°F		
1	2.665	148.2	I:	1.55
2	2.709	150.0	V:	48
3	2.734	151.0	T_f:	112°F
4	2.764	152.1	P_G:	22.75
5	2.615	146.	M:	10.0
6	out	----	P_B:	29.66
7	2.620	146.1	T_R:	73
8	2.00	120.8		
9	1.805	112.4		
10	1.810	112.5		
11	1.834	113.8		
12	2.216	122.0		
13	1.818	112.8		
14	2.124	126.0		
15	2.635	146.8		
16	2.615	146.0		
17	2.585	145.0		
18	2.620	146.20		
19	1.760	110.4		
20	1.716	108.5		

UNCORRECTED PERFORMANCE DATA

T. C. #	Millivolts Q = 135	°F		
1	3.17	169.0	I:	2.10
2	3.263	172.4	V:	64.5
3	3.330	174.8	T_f:	113°F
4	3.387	175.1	P_G:	19.70
5	3.0900	165.8	M:	10.0
6	out	----	P_B:	29.66
7	3.095	165.8	T_R:	72
8	2.310	133.5		
9	1.860	114.8		
10	1.885	115.5		
11	1.900	116.0		
12	2.492	141.0		
13	1.910	116.8		
14	2.388	136.8		
15	3.106	166.4		
16	3.080	165.2		
17	3.085	165.5		
18	3.095	166.0		
19	1.805	112.3		
20	1.765	110.5		

UNCORRECTED PERFORMANCE DATA

T. C. #	Millivolts Q = 159.0	°F		
1	3.37	176.4	I:	2.275
2	3.486	181.2	V:	70.0
3	3.570	184.4	T_f:	114°F
4	3.618	186.2	P_G:	18.20
5	3.266	172.4	M:	10.0
6	out	----	P_B:	29.66
7	3.250	172.0	T_R:	72
8	2.475	140.2		
9	1.915	117.0		
10	1.939	118.0		
11	1.955	118.8		
12	2.595	145.4		
13	2.01	120.8		
14	2.495	141.5		
15	3.265	172.4		
16	3.245	171.9		
17	3.245	171.9		
18	3.250	172.0		
19	1.841	113.9		
20	1.806	112.1		

UNCORRECTED PERFORMANCE DATA

T. C. #	Millivolts Q = 210	°F		
1	4.27	211.9	I:	2.60
2	4.366	215.10	V:	81
3	4.08	205.00	T_f:	112°F
4	out	----	P_G:	15.5
5	3.485	181.2	M:	10.0
6	out	----	P_B:	29.725
7	3.460	180.0	T_R:	73
8	2.73	150.8		
9	1.866	114.5		
10	1.887	116.0		
11	1.920	117.1		
12	2.660	148.0		
13	1.990	120.5		
14	2.560	144.0		
15	3.45	180.0		
16	3.43	179.0		
17	3.435	179.2		
18	3.438	179.5		
19	1.782	111.2		
20	1.765	110.4		

UNCORRECTED PERFORMANCE DATA

T. C. #	Millivolts Q = 259	°F		
1	out	----	I:	2.90
2	4.865	234.2	V:	89.5
3	4.550	222.4	T_f:	114°F
4	4.695	227.9	P_G:	13.20 13.30
5	3.710	189.9	M:	10.0
6	out	----	P_B:	29.725
7	3.682	189.0	T_R:	74
8	2.920	158.8		
9	1.900	114.4		
10	1.925	115.5		
11	1.970	118.2		
12	2.790	153.2		
13	2.045	122.5		
14	2.717	150.0		
15	3.626	186.5		
16	3.606	186.0		
17	3.612	186.1		
18	3.617	186.2		
19	1.814	112.8		
20	1.800	112.0		

UNCORRECTED PERFORMANCE DATA

T. C. #	Millivolts Q = 331.5	^{o}F	
1	out	----	I: 3.25
2	5.605	262.0	V: 102
3	5.195	246.8	T_f: 114^{o}F
4	5.360	253.0	P_G: 8.75
5	4.06	204.0	M: 10.0
6	out	----	P_B: 29.725
7	4.02	202.4	T_R: 76
8	3.17	169.0	
9	1.935	117.9	
10	1.945	118.4	
11	2.030	122.0	
12	2.985	161.2	
13	2.095	124.5	
14	2.975	161.0	
15	3.90	197.8	
16	3.88	197.0	
17	3.882	197.0	
18	3.890	197.5	
19	1.815	112.8	
20		112.8	

UNCORRECTED PERFORMANCE DATA

T. C. #	Millivolts Q = 353	^{o}F		
1	out	----	I:	3.35
2	5.78	268.2	V:	105
3	5.36	253.5	T_f:	115°F
4	5.52	259.0	P_G:	6.85
5	4.137	208.8	M:	10.0
6	out	----	P_B:	29.65
7	4.095	205.5	T_R:	78
8	3.210	170.1		
9	1.925	117.5		
10	1.947	118.2		
11	2.040	122.5		
12	3.070	164.8		
13	2.100	124.8		
14	3.025	163.0		
15	4.137	206.8		
16	4.050	202.5		
17	3.950	201.5		
18	3.965	201.6		
19	1.820	114.		
20	1.820	114.		

UNCORRECTED PERFORMANCE DATA

T. C. #	Millivolts Q = 44.2	°F		
1	2.931	159.2	I:	1.30
2	2.946	159.8	V:	34.0
3	2.930	159.4	T_f:	142°F
4	2.974	161.0	P_G:	21.20
5	2.881	157.0	M:	10.0
6	out	----	P_B:	29.69
7	2.894	157.8	T_R:	78
8	2.664	148.2		
9	2.580	144.8		
10	2.580	144.5		
11	2.580	144.5		
12	2.660	148.0		
13	2.578	144.5		
14	2.690	149.2		
15	2.915	158.4		
16	2.895	157.8		
17	2.886	157.5		
18	2.895	157.5		
19	2.531	142.4		
20	2.469	140.0		

UNCORRECTED PERFORMANCE DATA

T. C. #	Millivolts Q = 76.7	°F		
1	3.14	168.	I:	1.60
2	3.185	169.8	V:	48.0
3	3.21	170.2	T_f:	--
4	3.25	172.0	P_G:	20.4
5	3.086	165.4	M:	10.0
6	out	----	P_B:	29.85
7	3.079	165.0	T_R:	78
8	2.795	153.8		
9	2.545	143.20		
10	2.550	143.50		
11	2.55	143.50		
12	2.744	151.5		
13	2.58	143.50		
14	2.765	152.2		
15	3.10	166.0		
16	3.085	165.5		
17	3.085	165.5		
18	3.090	165.8		
19	2.50	141.2		
20	2.44	139.0		

UNCORRECTED PERFORMANCE DATA

T. C. #	Millivolts Q = 131.0	°F		
1	3.770	192.4	I:	2.075
2	3.924	198.5	V:	63.5
3	3.760	192.0	T_f:	--
4	3.600	186.0	P_G:	16.50
5	3.412	178.1	M:	10.0
6	out	----	P_B:	29.85
7	3.39	177.9	T_R:	76
8	2.972	160.8		
9	2.524	142.0		
10	2.536	142.8		
11	2.550	143.5		
12	2.855	156.0		
13	2.591	145.0		
14	2.890	157.2		
15	3.402	178.0		
16	3.385	177.2		
17	3.385	177.2		
18	3.395	177.8		
19	2.462	139.8		
20	2.410	137.9		

UNCORRECTED PERFORMANCE DATA

T. C. #	Millivolts Q = 149	°F		
1	4.13	206.5	I:	2.21
2	4.191	209.0	V:	67.5
3	3.961	200.0	T_f:	--
4	3.840	195.2	P_G:	15.40
5	3.490	181.8	M:	10.0
6	out	----	P_B:	29.85
7	3.485	181.0	T_R:	76
8	3.065	164.5		
9	2.572	144.2		
10	2.585	144.8		
11	2.602	145.5		
12	2.904	158.0		
13	2.640	147.2		
14	2.955	161.9		
15	3.49	181.8		
16	3.475	180.8		
17	3.475	180.8		
18	3.485	181.0		
19	2.515	142.0		
20	2.464	140.0		

UNCORRECTED PERFORMANCE DATA

T. C. #	Millivolts Q = 197	°F		
1	4.457	219.2	I:	2.525
2	4.665	226.5	V:	78.
3	4.400	216.5	T_f:	--
4	4.400	216.5	P_G:	12.35
5	3.73	191.0	M:	10.0
6	out	----	P_B:	29.85
7	3.71	190.0	T_R:	75
8	3.215	170.2		
9	2.560	144.0		
10	2.575	144.2		
11	2.60	145.8		
12	3.025	163.2		
13	2.645	146.5		
14	3.135	167.5		
15	3.695	189.5		
16	3.675	188.5		
17	3.680	188.8		
18	3.685	189.0		
19	2.487	140.8		
20	2.490	141.0		

UNCORRECTED PERFORMANCE DATA

T. C. #	Millivolts Q = 256	^{o}F		
1	out	----	I:	2.86
2	5.12	244.	V:	89.5
3	4.88	235.0	T_f:	--
4	4.96	239.0	P_G:	8.05
5	4.048	203.8	M:	10.0
6	out	----	P_B:	29.85
7	4.005	201.9	T_R:	75
8	3.455	179.8		
9	2.589	145.0		
10	2.600	145.2		
11	2.650	147.8		
12	3.164	168.8		
13	2.685	149.0		
14	3.305	174.0		
15	3.960	200.2		
16	3.950	200.0		
17	3.950	200.0		
18	3.955	200.1		
19	2.500	141.3		
20	2.462	140.0		

UNCORRECTED PERFORMANCE DATA

T. C. #	Millivolts Q = 297.6	^{o}F		
1	out	----	I:	3.10
2	5.420	255.2	V:	96
3	5.000	239.5	T_f:	--
4	5.350	252.5	P_G:	4.05
5	4.225	210.0	M:	10.0
6	out	----	P_B:	29.85
7	4.205	209.5	T_R:	73.5
8	3.60	186.0		
9	2.59	145.2		
10	2.612	146.0		
11	2.662	148.0		
12	3.30	174.0		
13	2.705	149.9		
14	3.505	183.9		
15	4.152	207.8		
16	4.140	207.2		
17	4.140	207.2		
18	4.145	207.3		
19	2.50	141.5		
20	2.465	140.0		

UNCORRECTED PERFORMANCE DATA

T. C. #	Millivolts Q = 359	^{o}F		
1	out	----	I:	3.40
2	5.885	272.1	V:	105.5
3	5.420	255.4	T_f:	--
4	5.665	264.0	P_G:	1.00
5	4.465	219.0	M:	10.0
6	out	----	P_B:	29.85
7	4.444	218.1	T_R:	73
8	3.755	192.4		
9	2.576	144.4		
10	2.600	145.5		
11	2.670	148.1		
12	3.425	178.8		
13	2.715	150.0		
14	3.735	191.0		
15	4.375	215.8		
16	4.357	215.0		
17	4.357	215.0		
18	4.366	215.5		
19	2.480	140.2		
20	2.450	139.50		

APPENDIX D

(1.) Thermocouple Conduction Error Correction

Because the thermocouples in the cooling jacket had wires exposed to a crossflow of a moving fluid, a conduction error existed. An error in reading would occur because the wire, acting as a fin, would conduct heat from the surface causing a local "cold" spot. This would lead to an erroneously lower value in the measured temperature.

Schneider (10) developed a method for correcting these errors. His development applied to this investigation leads to the expression:

$$\frac{T_i - T_\infty}{T_f - T_i} = \frac{\left(K_1^t + \frac{q_c \pi r_s^2}{T_f - T_i} \right) K_0\left(r_s \sqrt{\frac{h_1}{K\delta}} \right)}{2\pi K \delta r_s \sqrt{\frac{h_1}{K\delta}} \; K_1\left(r_s \sqrt{\frac{h_1}{K\delta}} \right)} \qquad (1.)D$$

A sample calculation follows.

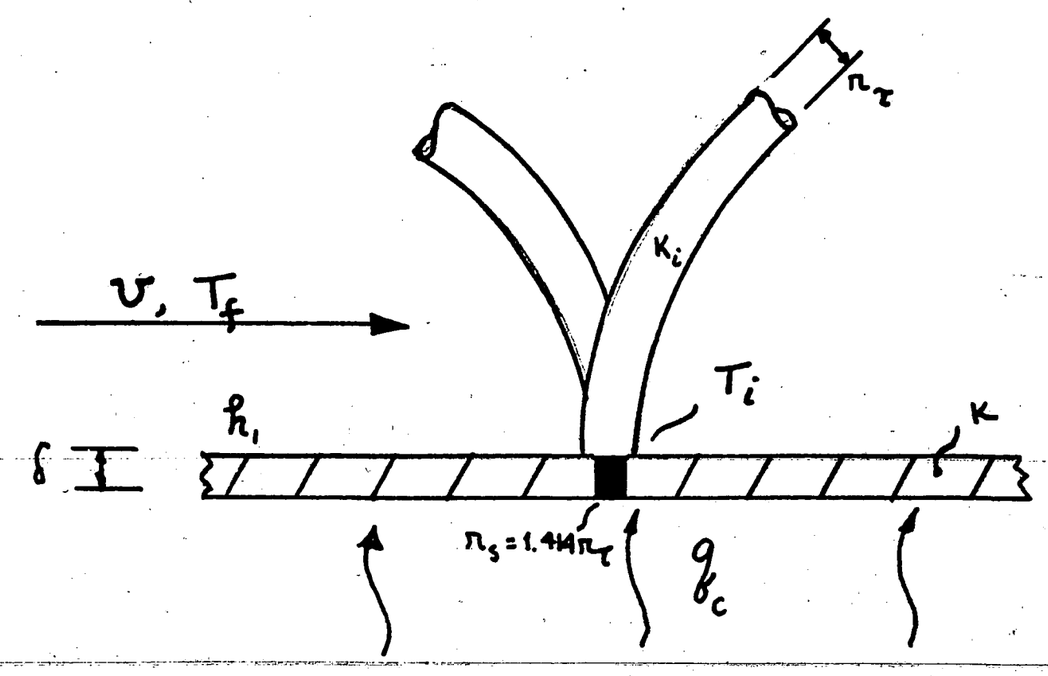

$D_T = .00167$ FT.

$\delta = .0052$ FT.

$r_s = .00236$ FT.

$T_\infty =$ CORRECT TEMPERATURE

$T_f = 60°F.$

PR. NO. = 8.03

$\rho = 62.3\ \#_m / FT.^3$

$\nu = 1.22\ FT.^2/SEC.\ (x10^{-5})$

$\upsilon = .214\ FT./SEC.$

$$R_e = \frac{\upsilon D}{\nu} = \frac{.214\ FT/SEC. \times .00167\ FT.}{1.22 \times 10^{-5}\ FT^2/SEC.}$$

$R_e = 29.2$

ASSUME CONDUCTION ENTIRELY IN COPPER WIRE

$k = 200\ \frac{BTU}{HR.FT\ °F}$

$A = 2.19 \times 10^{-6}\ FT.^2$

$P = .00525\ FT.$

$K_f = .34\ \frac{BTU}{HR.FT.\ °F}$

NOW,

$$\frac{h_c D_o}{K_f} = 1.1C \left(\frac{U_f D}{\nu_f}\right)^m P_R^{.31}$$

$C = .821$; $m = .385$

EVALUATING,

$$h_c = 1295 \ \frac{BTU}{HR.\ FT.\ ^\circ F}$$

NOW,

$$K_1^t = \sqrt{h P k A} \ \ TANH\ ml$$

BUT,

$$TANH\ ml \approx 1.0$$

AND,

$$K_1^t = \sqrt{h P k A}$$

$$= \sqrt{1295 \frac{BTU}{HR.\ FT^2\ ^\circ F} \times .00525\ FT \times 200 \frac{BTU}{HR\ FT\ ^\circ F} \times 2.19 \times 10^{-6} FT^2}$$

$$= \sqrt{29.8 \times 10^{-4} \frac{BTU^2}{HR^2\ ^\circ F^2}}$$

$$K_1^t = .0545 \ \frac{BTU}{HR.\ ^\circ F}$$

IF $q_c = 300$ WATTS $= 1030 \ \frac{BTU}{HR}$

AND $T_f - T_{in} = -5^\circ F$

THEN

$$\frac{q_c \pi r_s^2}{(T_f - T_i) A_s} = \frac{1030 \times \pi \times (.00236)^2}{(-5) \times .285}$$

$$= 12.7 \times 10^{-3} \frac{BTU}{HR\ ^\circ F}$$

h_1 MUST NOW BE EVALUATED

$D_1 = 1.31$ IN. (OUTSIDE DIAMETER OF PIPE.)

$D_2 = 2.00$ IN. (INSIDE DIAMETER OF COOLING JACKET OUTER BRASS PIPE.)

$\dot{m} = 10\ \#m/min$

$T_f = 60\ ^\circ F$

FROM CONTINUITY : $\dot{m} = \rho A v$

$v = .214 \frac{FT.}{SEC.}$

ALSO,

$R_e = 1010$: LAMINAR

FROM KREITH (8), FIG. 8-12, PG. 390.

WITH,

$$\frac{Re\ Pr\ D_H}{L} = \frac{1010 \times 8.03 \times .69}{10} = 558$$

$$\overline{Nu_D} = 20.0$$

AND ∴

$$h = 62.5 \frac{BTU}{FT.^2 HR.\,^\circ F}; K = 9 \frac{BTU}{HR.FT\,^\circ F}$$

$$\epsilon = \sqrt{\frac{h_1}{K\delta}} = \sqrt{\frac{62.5}{9 \times .0052}} = 36.4\ FT.^{-1}$$

$$\epsilon \pi_s = .0860 \approx .10$$

$$K_0(.10) \Big/ K_1(.10) = .246$$

SUBSTITUTING INTO $(1.)_D$

$$\frac{T_i - T_{\infty}}{T_f - T_i} = .655$$

FOR $T_f = 150°F$

$$\frac{T_i - T_\infty}{T_f - T_i} = .61$$

FOR OTHER VALUES OF $\frac{q}{c}$, $T_f - T_i$

A REPRESENTATIVE AVERAGE IS,

$$\frac{T_i - T_\infty}{T_f - T_i} = .600$$

IF $T_f = 50°F$

$$T_i = T_{10} = 60.0°F$$

$$T_{10} - T_\infty = (-10.0).60 = -6.00$$

$$T_\infty = T_{10} + 6.0$$

FINALLY,

$$T_\infty = 60.0 + 6.0 = 66.°F$$

APPENDIX E

CLEANING PROCESS

The cleaning process described below for the stainless steel heat pipe and parts was developed at Western Electric Company in Allentown, Pennsylvania.

I. Trichloroethylene Degrease

1.) Degreaser #1

Vapor degrease for 5 minutes above boiling section of ultrasonic degreaser and for 5 minutes in the boiling ultrasonic fluid.

2.) Degreaser #2

(a much cleaner degreaser)

Vapor degrease for 5 minutes and ultrasonic degrease for 5 minutes.

II. Rinse

Using overflowing distilled water

III. Clean #1

Use ethyl alcohol, H_2O_2 & NaOH solution

IV. Rinse

Overflowing distilled water

V. Clean #2

Hydrochloric acid solution (5 minutes)

VI. Rinse

Overflowing distilled water

VII. Clean #3

Nitric acid solution

VIII. Rinse

Overflowing distilled water

IX. Ultrasonic Distilled Water Rinse (5 minutes)

X. Acetone Dip and Hot Air Dry

Solutions:

Clean #1 800 cm^3 warm distilled water

200 cm^3 190 proof ethyl alcohol

50 cm^3 30% H_2O_2

100 gms. NaOH

Clean #2 18.5 liters distilled water

1.85 liters concentrated hydrochloric acid

Clean #3 800 cm^3 distilled water

400 cm^3 concentrated nitric acid

APPENDIX F

(1.) Permeability Experiment

Permeability is defined as the ability of a substance to allow another substance, especially a fluid, to pass through itself.

The term used to describe the permeability phenomenon in heat pipes is called the permeability characteristic, b, which is dimensionless. The permeability characteristic is defined by the following equation:

$$b = \left[\frac{A_w}{L}\right]\left[\frac{\rho_L}{\mu_L}\right]\left[\frac{\Delta P_L}{\dot{M}_L}\right]\left[r_c^2\right]$$

It is the flow of the fluid through the many interconnected pores and channels of the wick that causes a friction pressure drop ΔP_L.

In the operation of a heat pipe the permeability characteristic, b, is the only value that cannot be determined from the operation of the pipe. If the limitations of the pipe, due to pumping capacity, are to be calculated, it is essential that b be evaluated. It is necessary, then, to simulate the fluid return of the pipe by a device and determine the value b.

The device used to evaluate b was simply two plexiglass plates 8"x3"x1/4", 10 layers of the same wire cloth used in the pipe, springs, caulking, a clamping device, and a micrometer.

The wire cloth (6"x2"x.01" per layer) was placed between two plates. The plates were spaced apart by springs in each corner. A clamping stand consisting of a

rectangular steel structure with 1/4" screws was used to tighten and fix the plexiglass and wire cloth to a proper dimension. This dimension was measured with a micrometer. Caulking was used to seal the sides of the wire cloth and, thus, insure flow only through the wicking. Plexiglass shims were glued to the sides so that the device could be removed from the clamping stand.

Figure (23) describes the permeability experiment. A pressure head was set with the graduated cylindrical tank and a mass flow measured. A graph of ΔP versus $\dot{M}$ could be plotted and, since the flow being Darcian, the resulting plot would be linear. The slope of the curve would be a constant value. If one inspects the equation at the beginning of this section, it can be observed that this slope times and constant geometry constant is the value b. So, b is constant for a given fluid, capillary structure, and specified dimensions.

The fluid used was distilled water and the tightness of the wicking was set so that the dimension measured was equivalent to 10 wire cloth layers. The result is plotted in Figure (24) and the value is calculated to be approximately 42. The value of permeability was initially constant with time, but increased in magnitude after a certain amount of flow passed through the wicking material. This same phenomenan was reported by Ginwala, Blatt, and Bilger (11) and in a NASA report (12) prepared by Pratt and Whitney. This effect is attributed to gas

bubbles present in the liquid in the material.

It was also attempted to vary the thickness of the wicking so that a family of curves could be obtained and that a value of b representative to the tightness of the heat pipe wicking could be obtained.

This attempt, however, failed. The Pratt and Whitney study investigated several wickings and fluids. Using their sample of M2 with a porosity of 64.5%, a pore radius of a 100 microns, and a wick friction factor of 3.4×10^{8} Ft.$^{-2}$, a value of b is calculated to be approximately 35.5 which is surprisingly close to that of the wire cloth used in this investigation.

(2.) Permeability Results

#F/in^2	#/min.
.515	.1235 .1120
.467	.1070
.431	.0960 .0858
.396	.0810
.359	.0690 .0675
.323	.0595
.287	.0495 .0500
.251	.0410
.216	.0335 .0315
.179	.0270
.143	.0210 .0185
.072	.0085

A_c = .363 in.^{2}

L = 6 in.

APPENDIX G

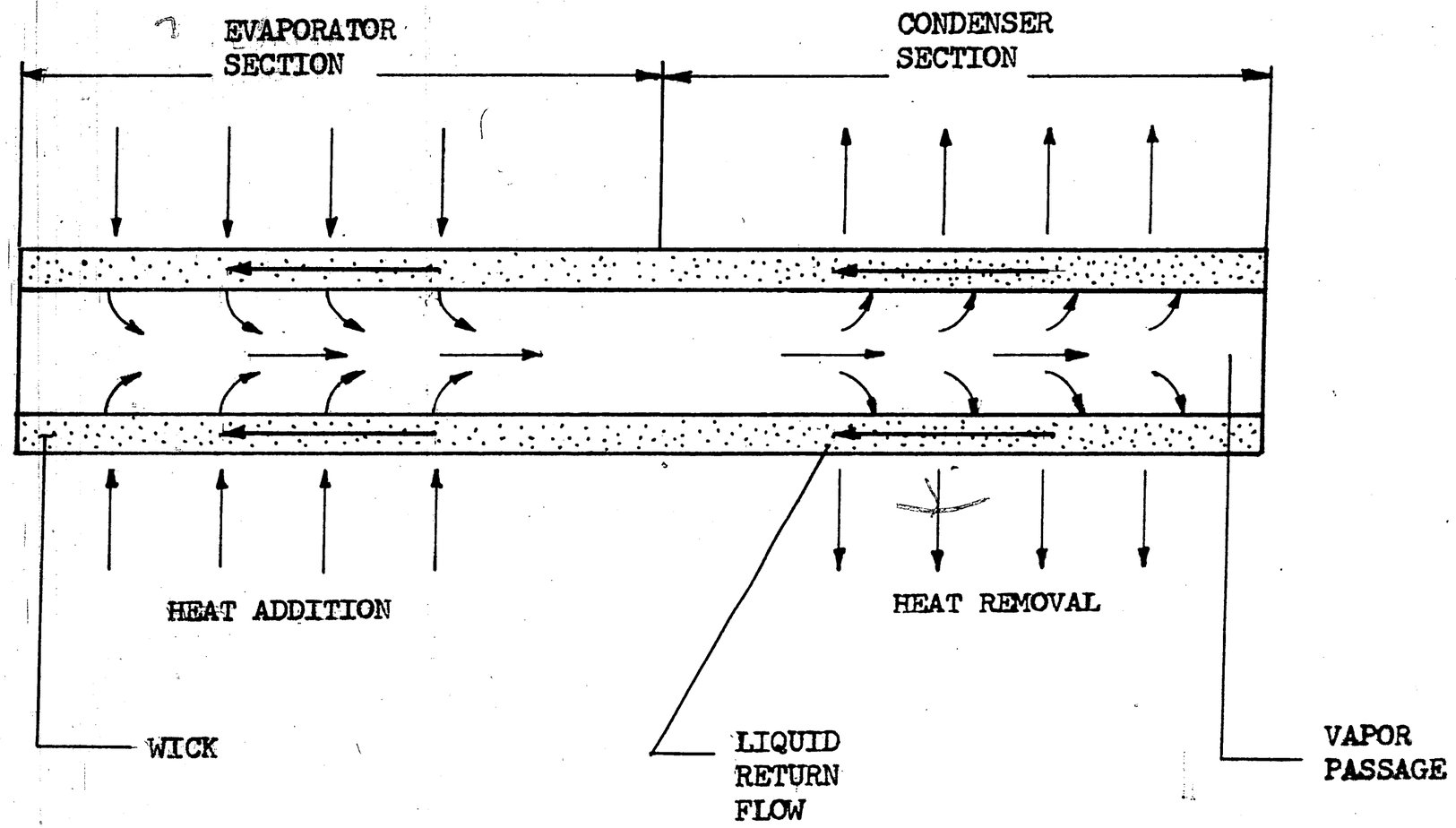

FIGURE 1. BASIC HEAT PIPE DEVICE

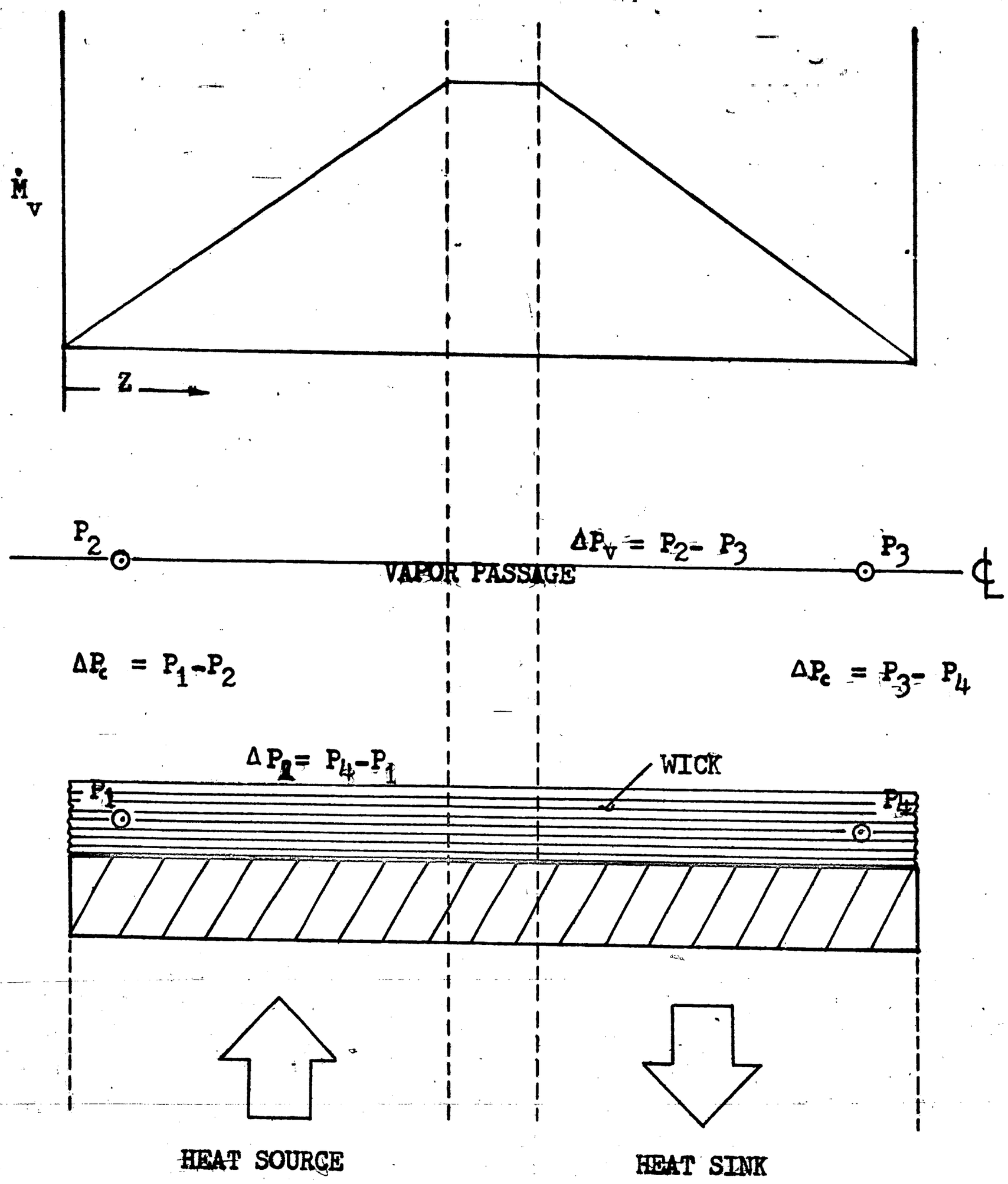

FIGURE 2. SCHEMATIC OF VAPOR MASS FLOW AND PRESSURE DROPS

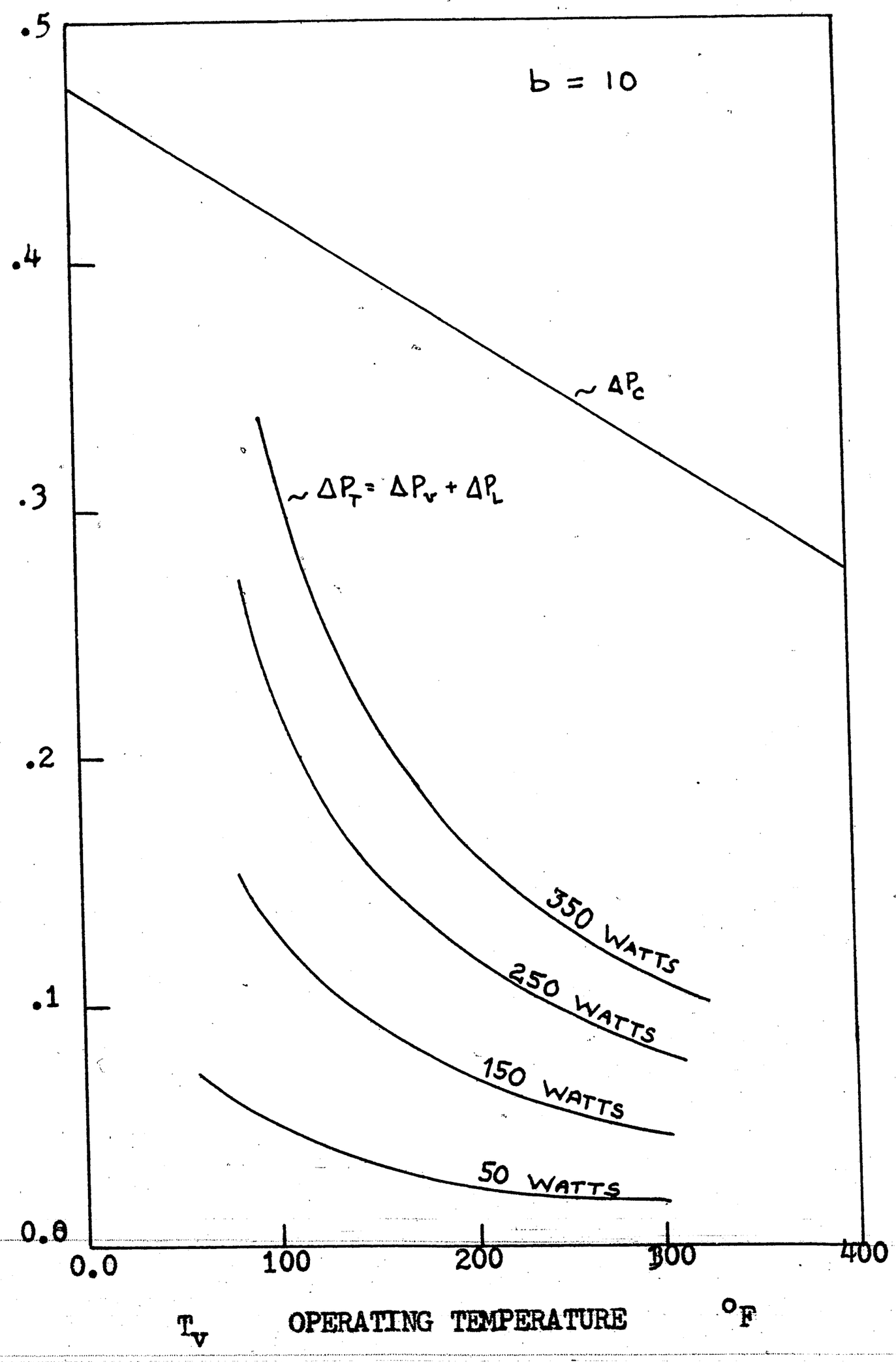

FIGURE 3. THEORETICAL PRESSURE-TEMPERATURE PERFORMANCE CURVE

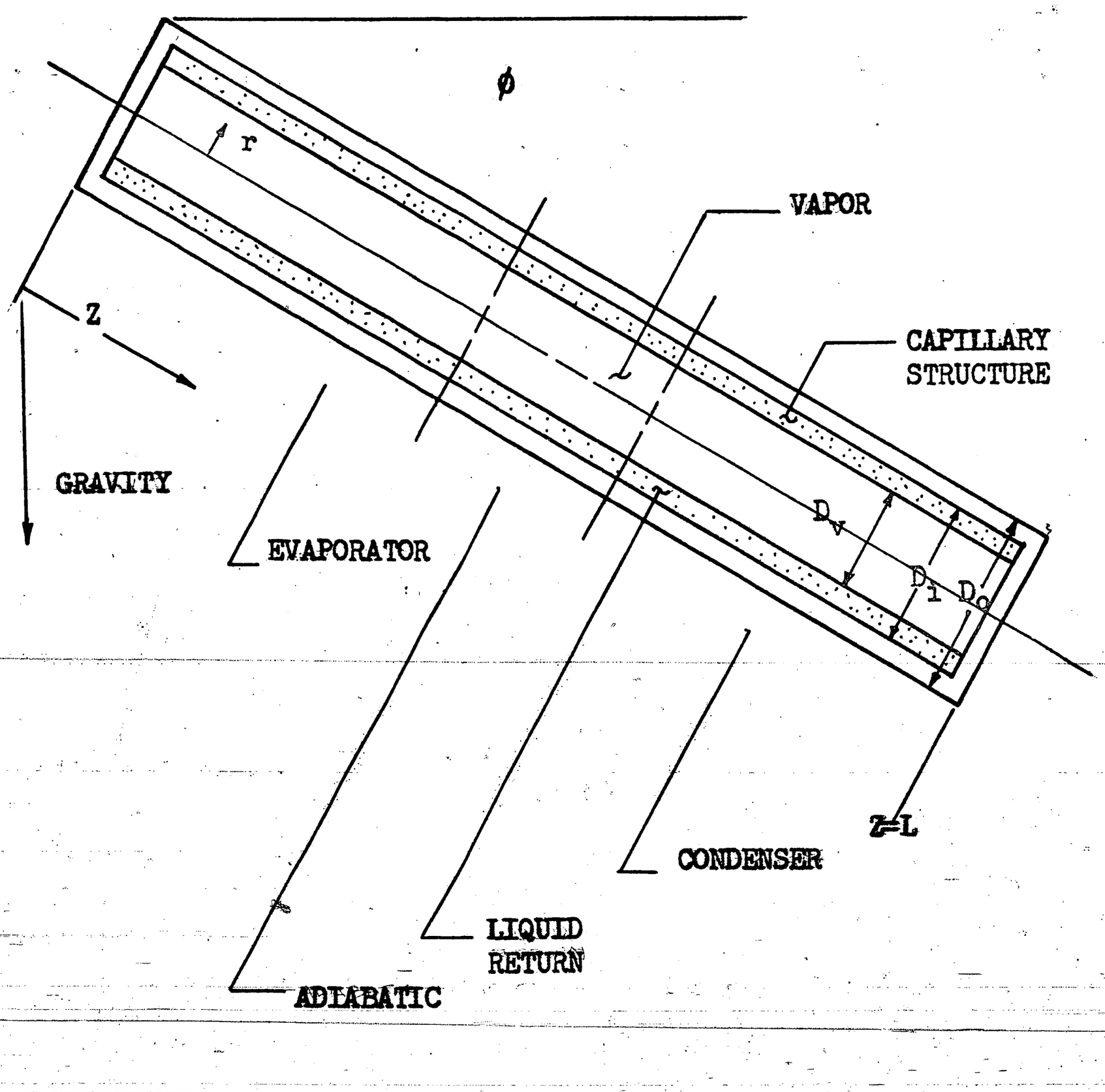

FIGURE 34. GENERAL COORDINATE SYSTEM

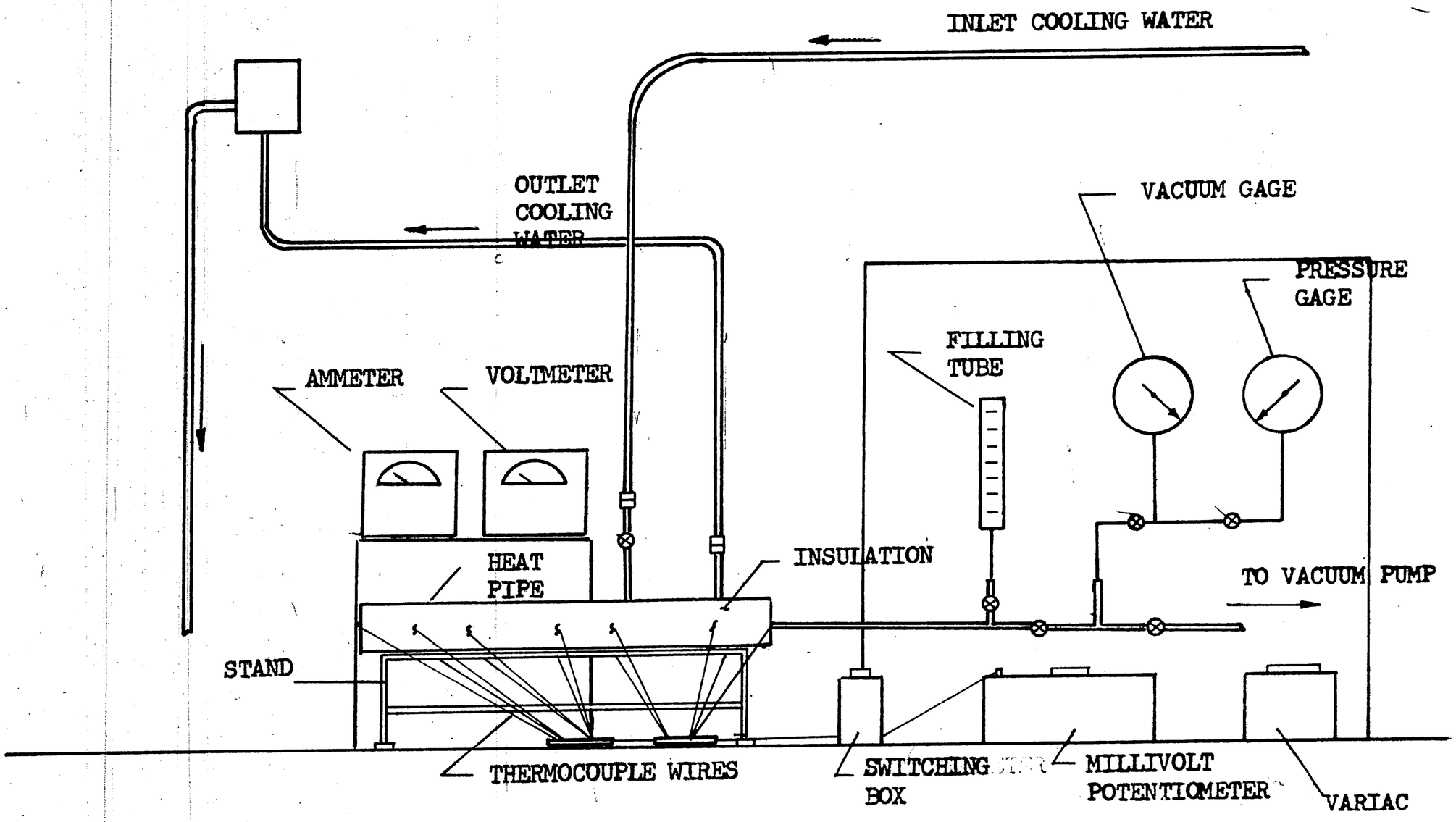

FIGURE 5. HEAT PIPE APPARATUS

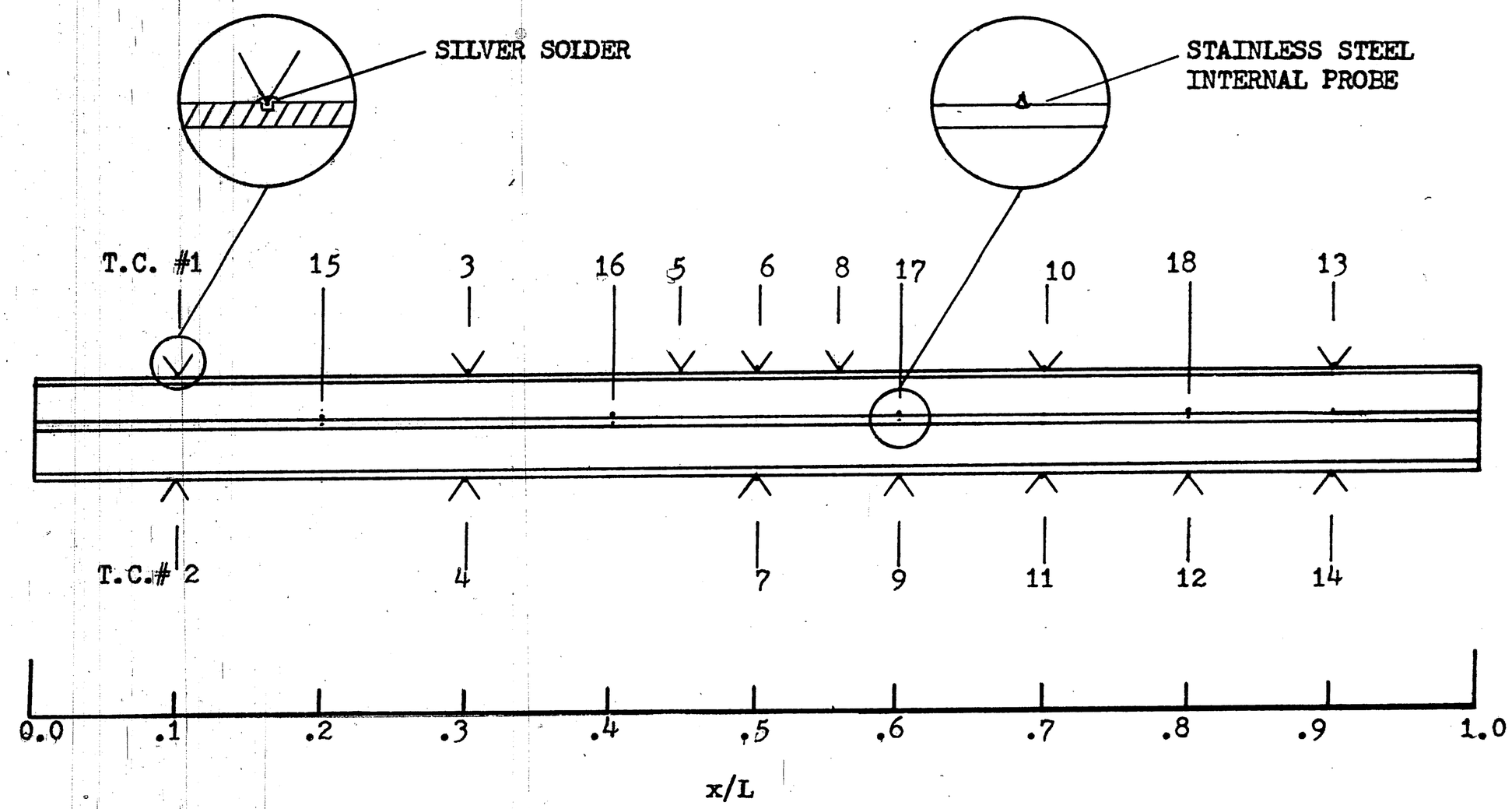

FIGURE 6. THERMOCOUPLE POSITIONS

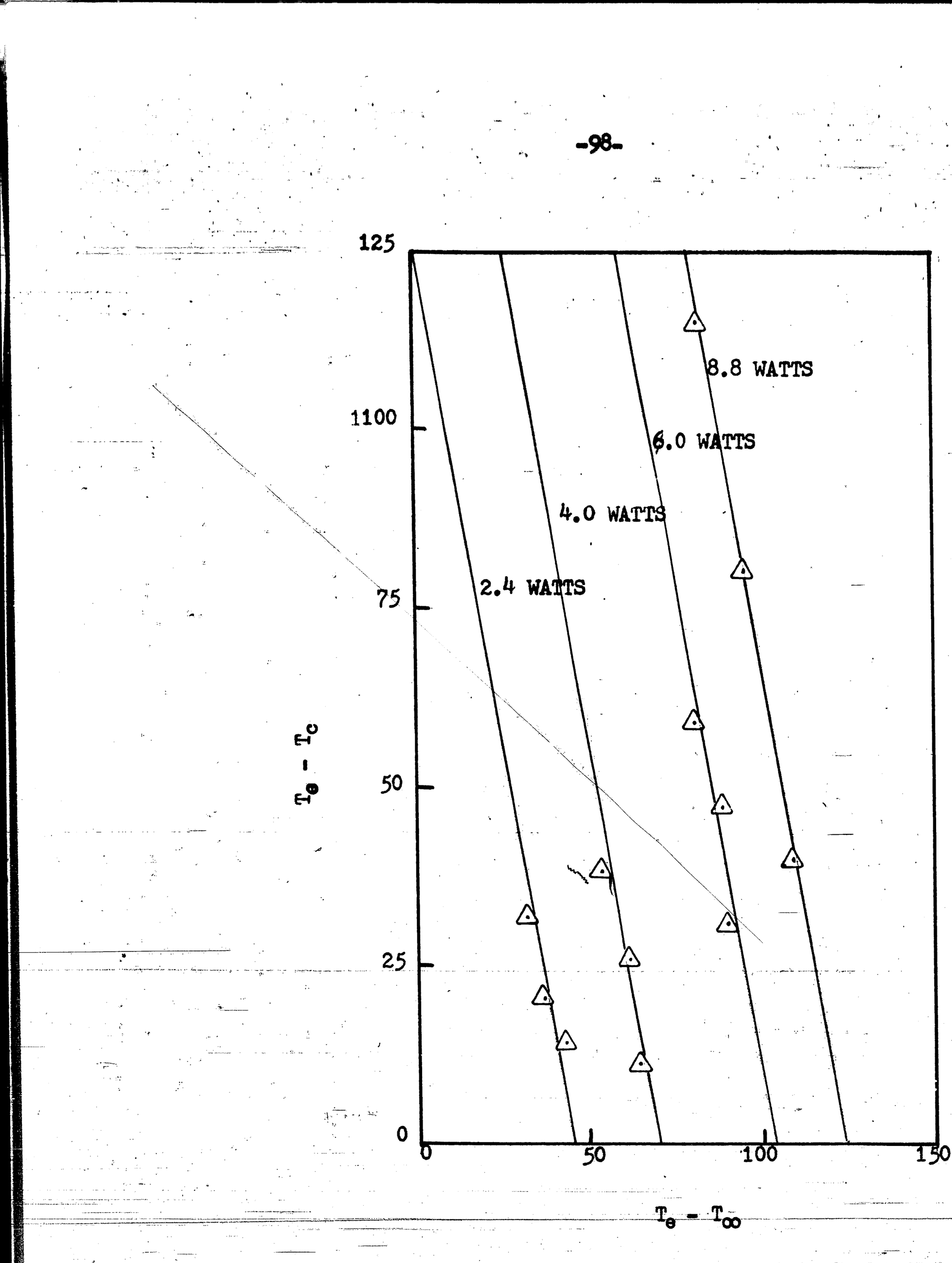

FIGURE 7. HEAT LOSS CALIBRATION CURVE

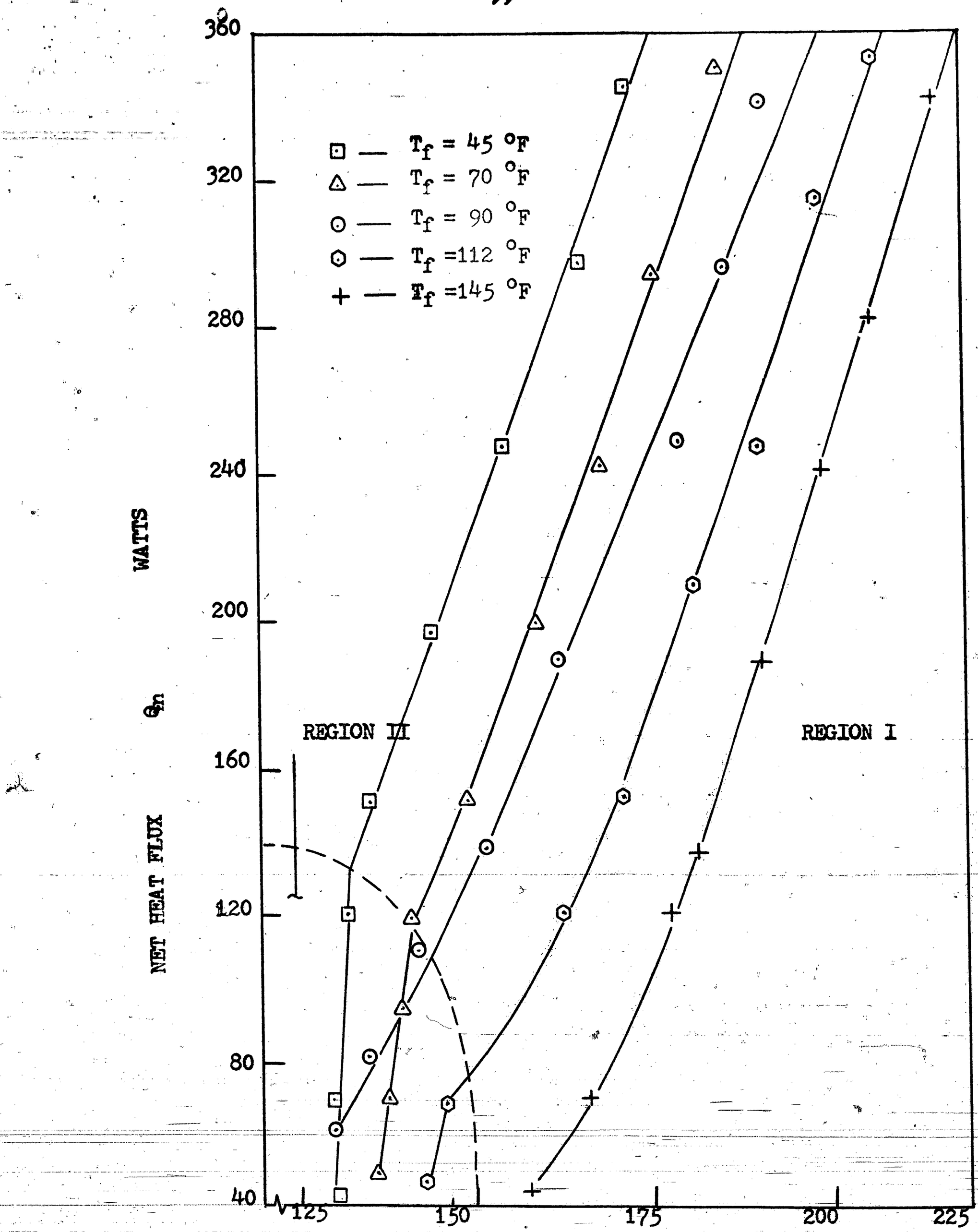

FIGURE 8. POWER - TEMPERATURE PERFORMANCE CURVE

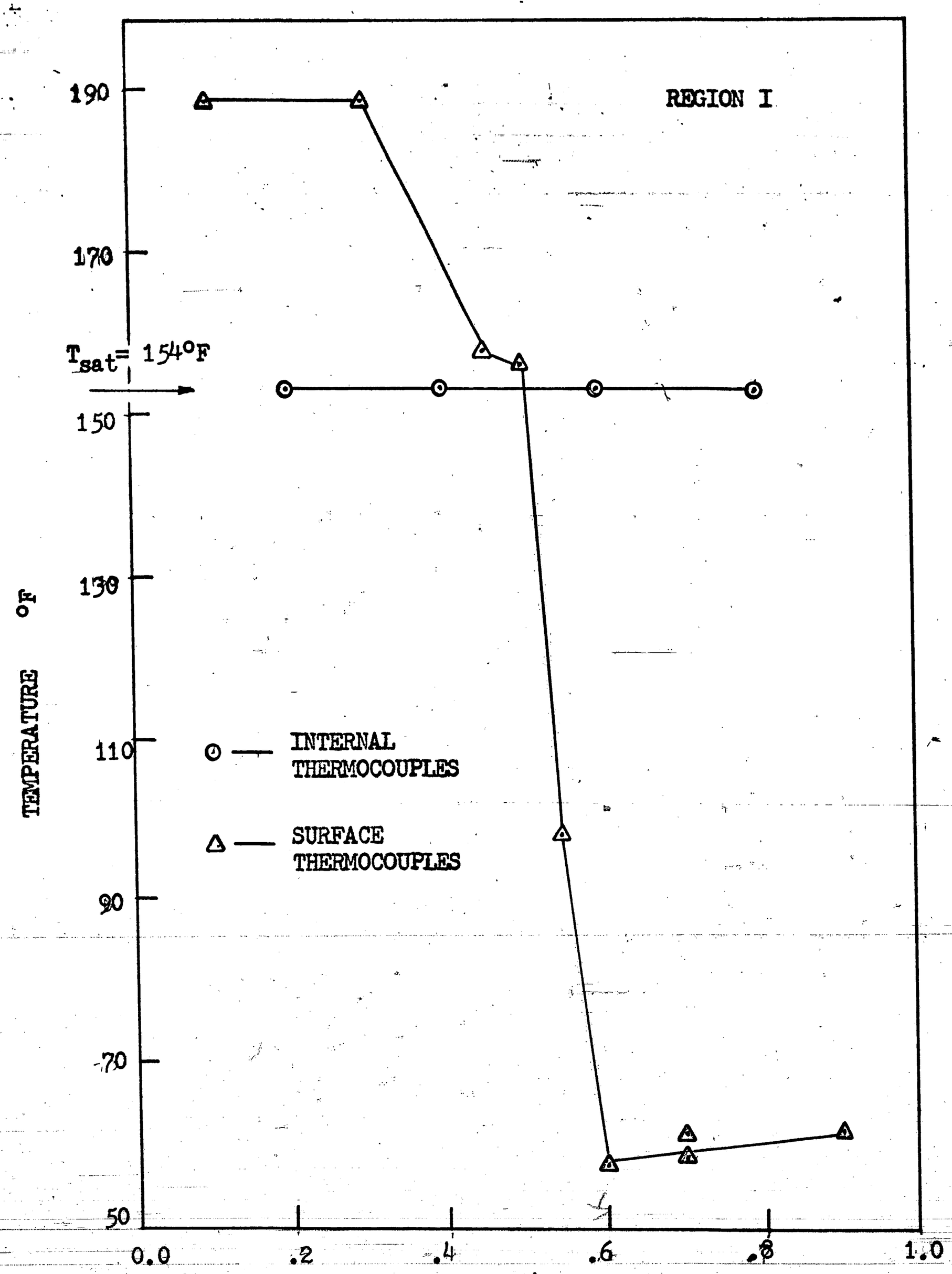

FIGURE 9. TEMPERATURE PROFILE Q=248 WATTS, T_f = 48 °F

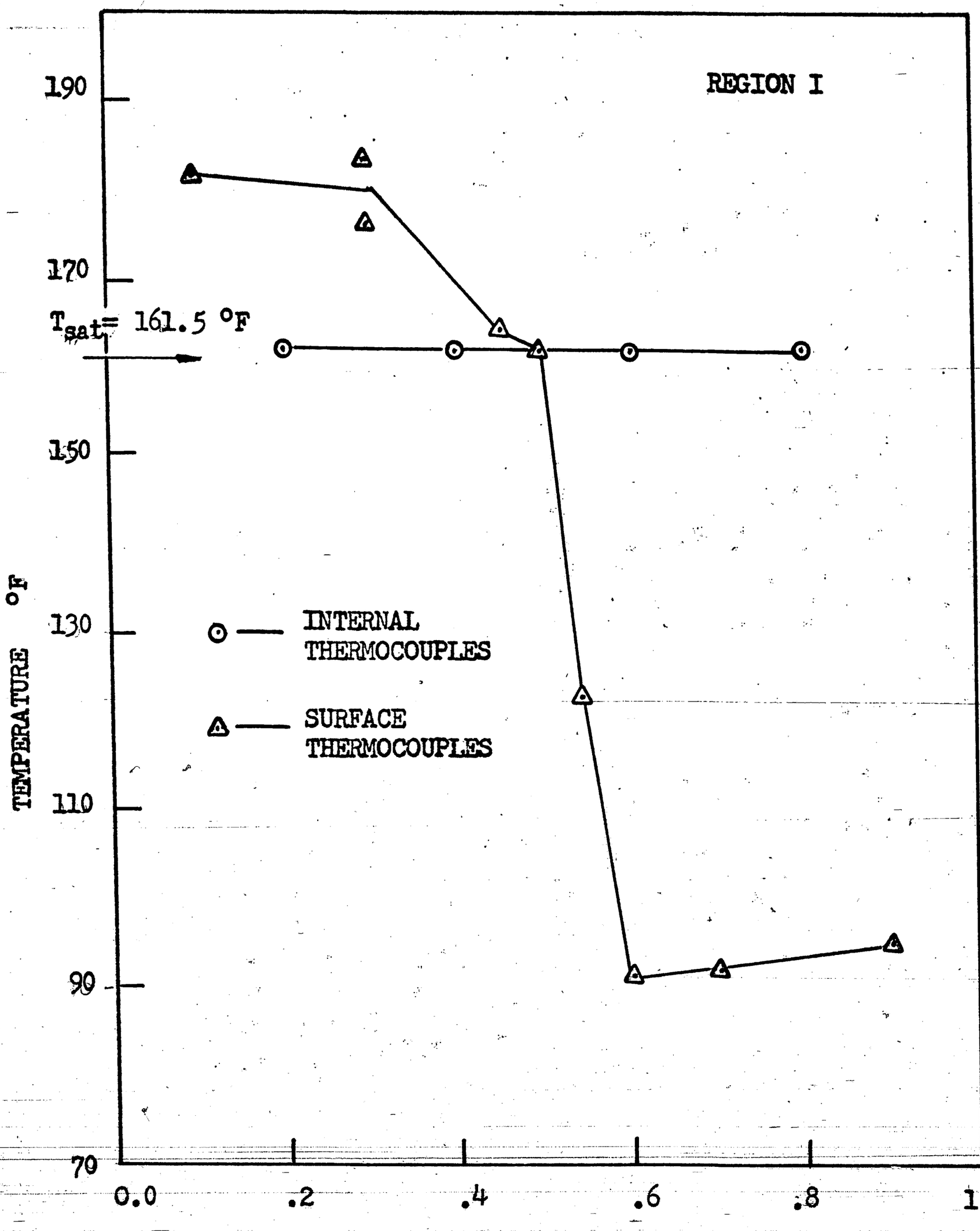

FIGURE 10. TEMPERATURE PROFILE Q=190 WATTS, T_f= 88 °F

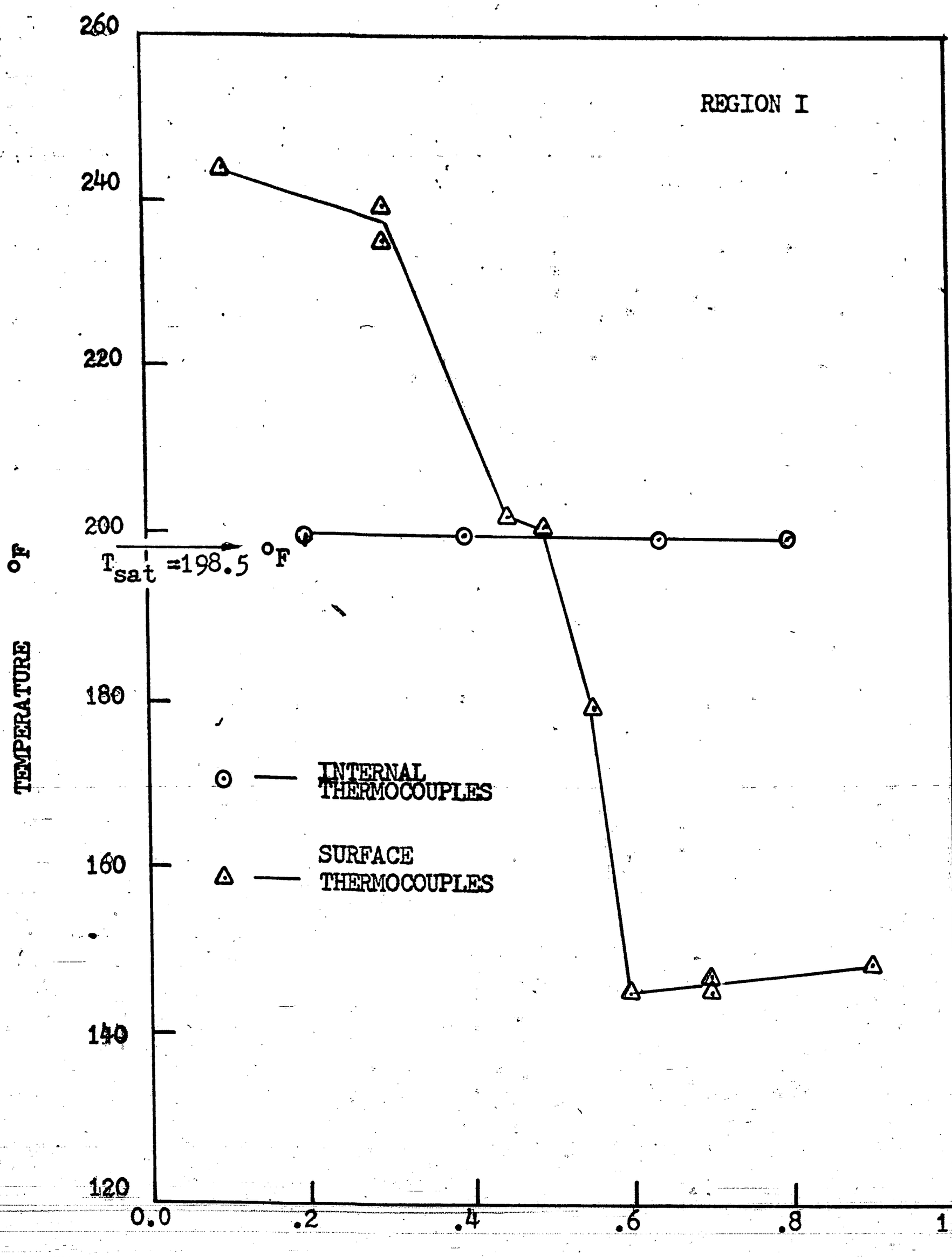

FIGURE 11. TEMPERATURE PROFILE Q=243 WATTS, T_f= 140 °F

FIGURE 12. TEMPERATURE PROFILE Q=71 WATTS, T_f= 70 °F

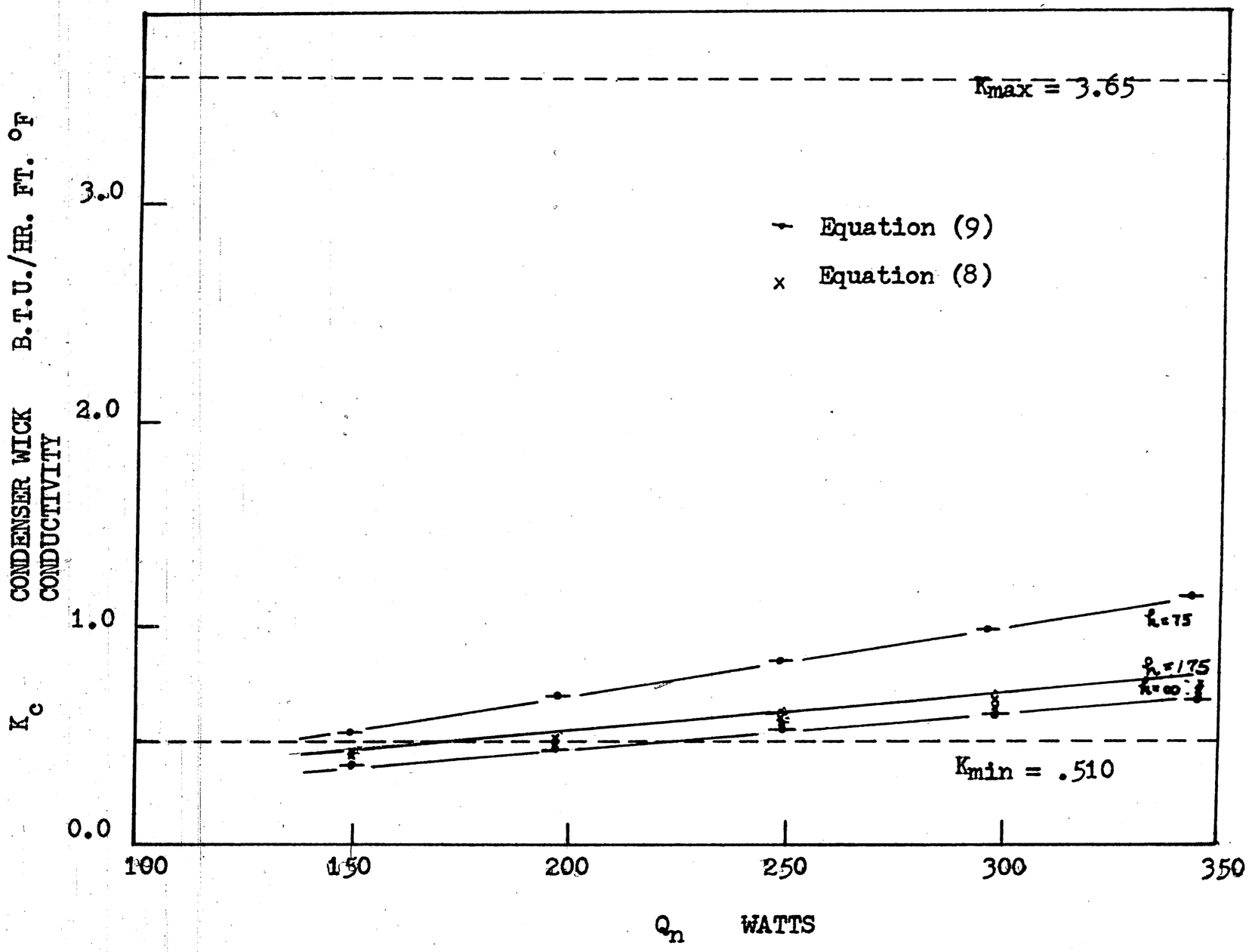

FIGURE 13. CONDENSER WICK CONDUCTIVITY, $T_f = 45$ °F

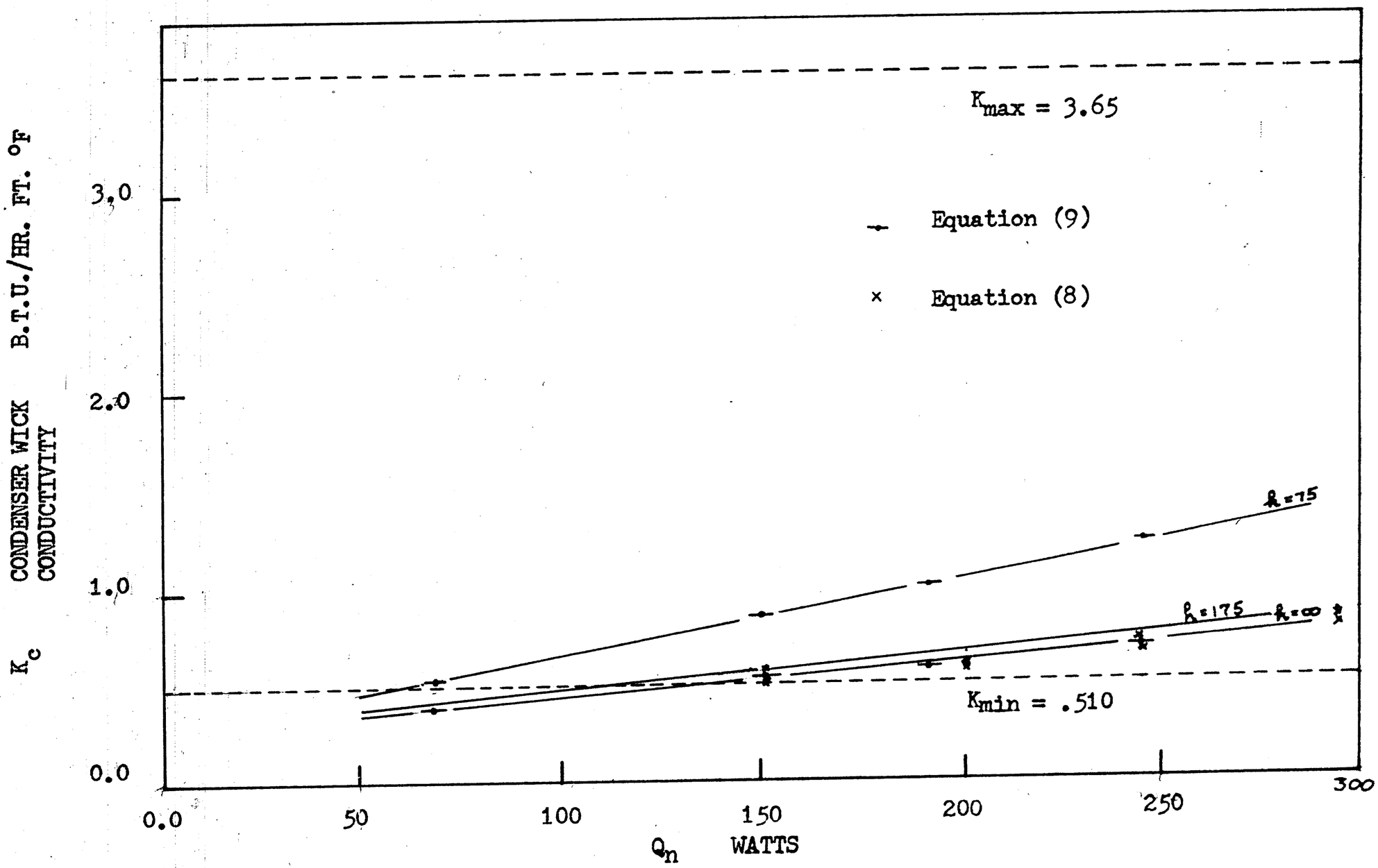

FIGURE 14. CONDENSER WICK CONDUCTIVITY, T_f = 70 °F

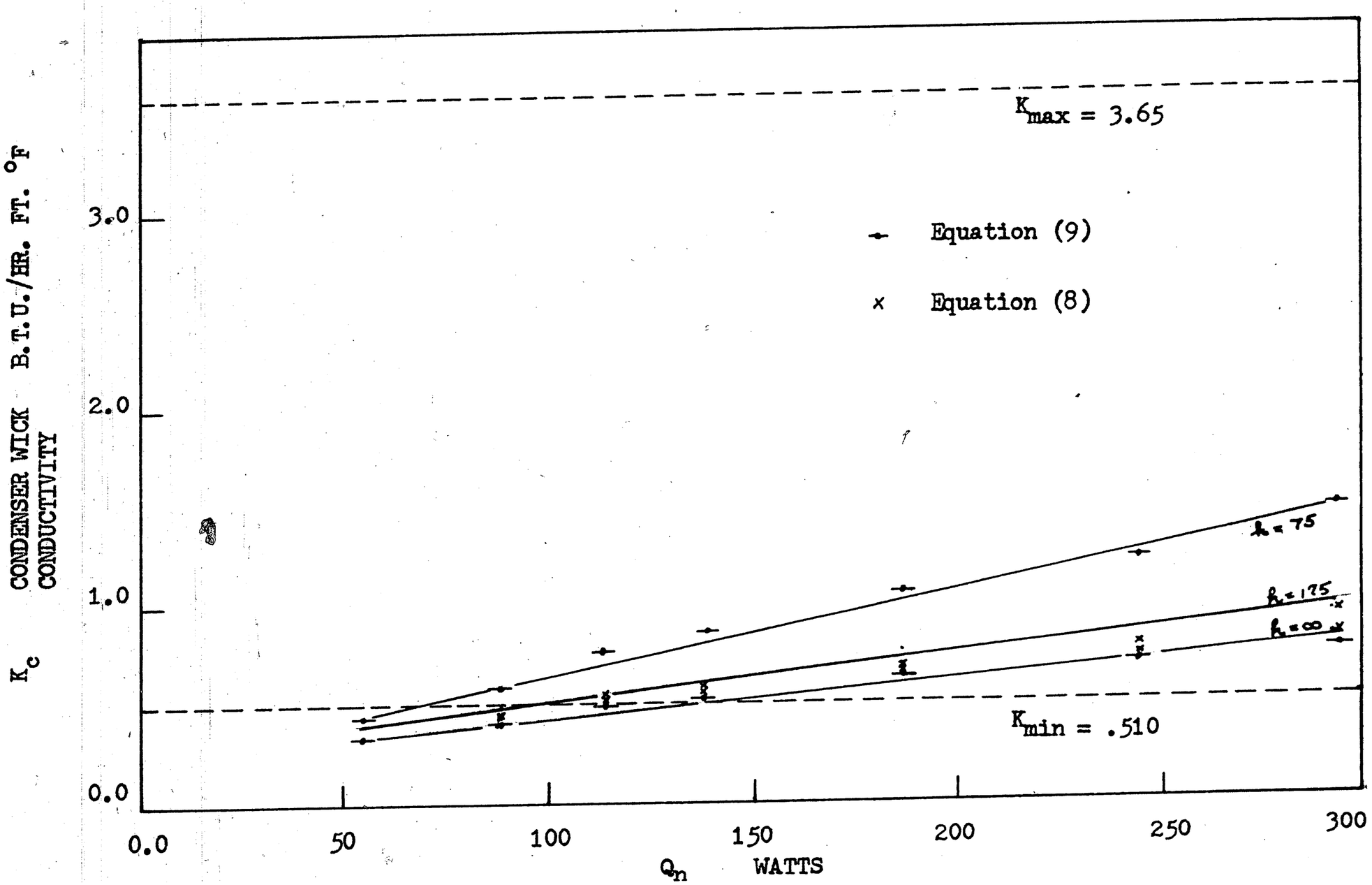

FIGURE 15. CONDENSER WICK CONDUCTIVITY , T_f = 90 °F

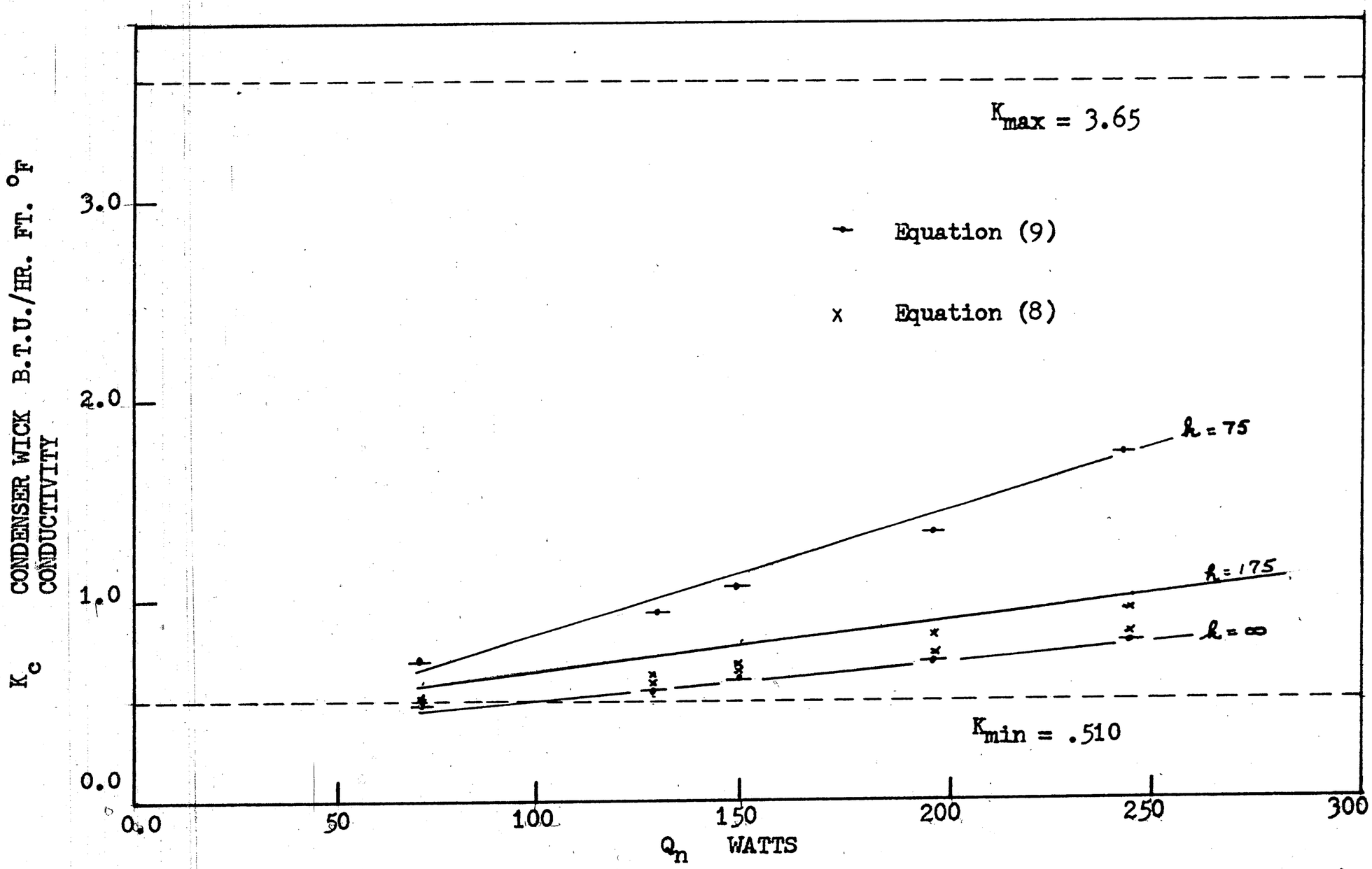

FIGURE 16. CONDENSER WICK CONDUCTIVITY, T_f = 112 °F

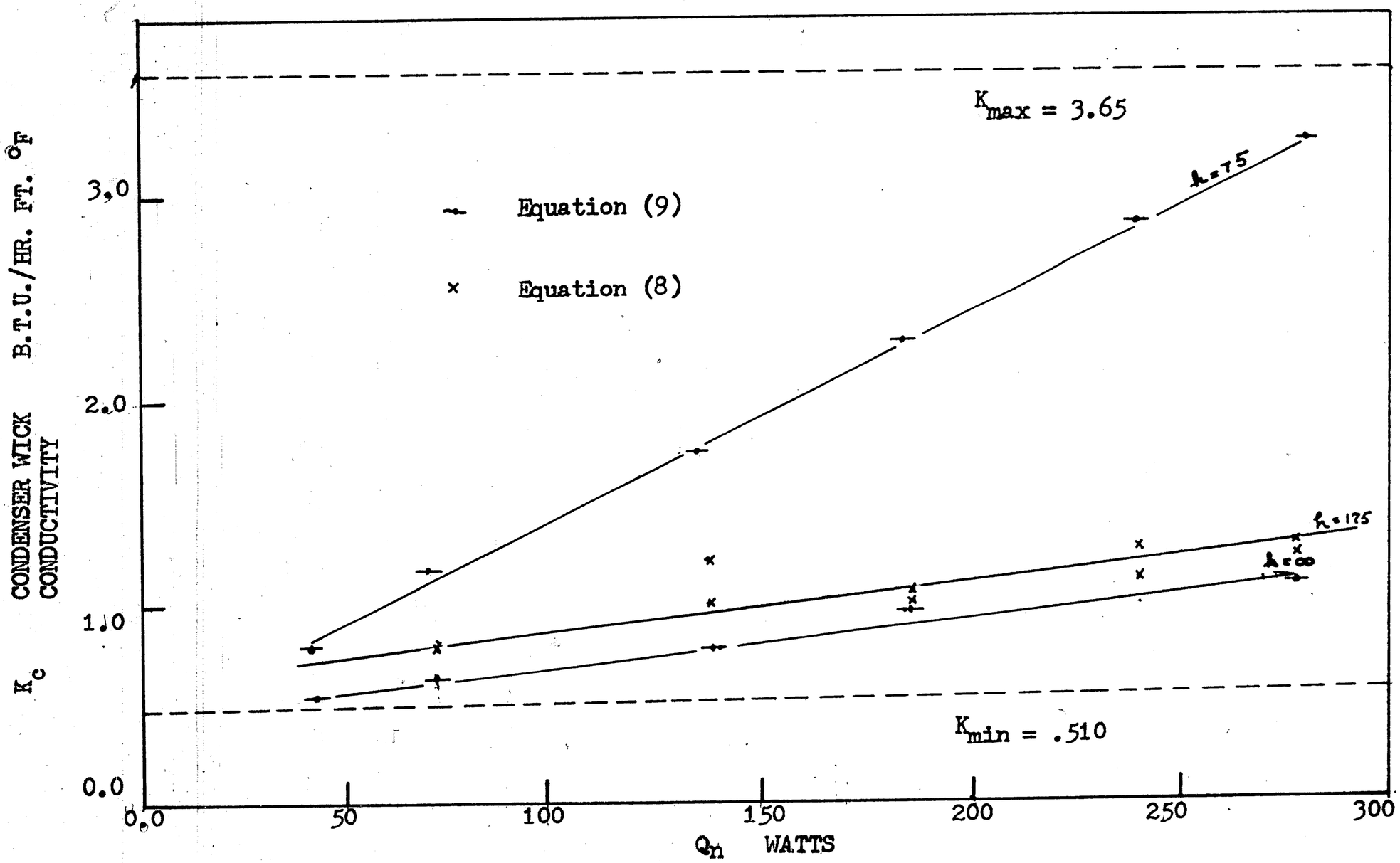

FIGURE 17. CONDENSER WICK CONDUCTIVITY, T_f = 140 °F

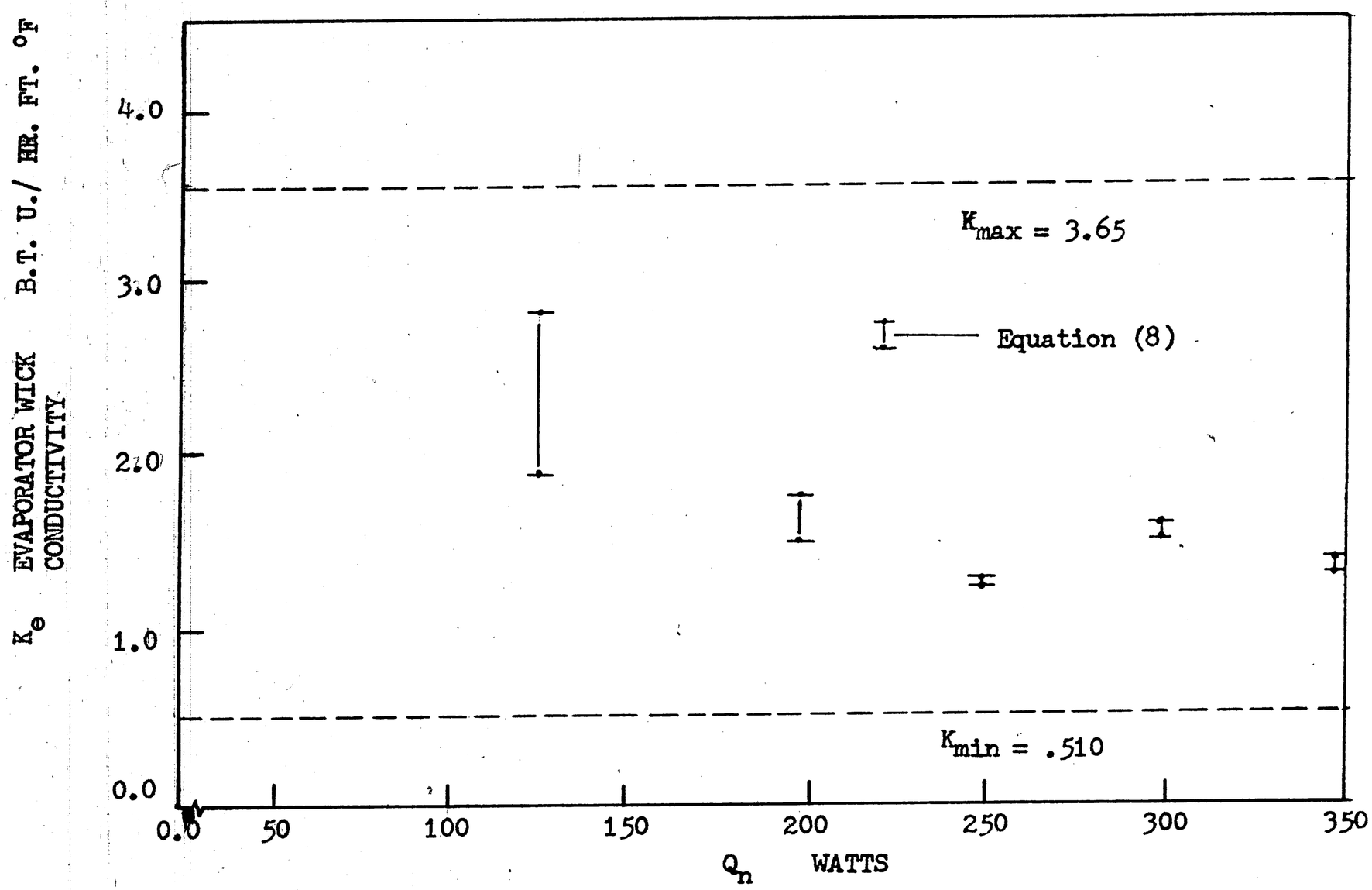

FIGURE 18. EVAPORATOR WICK CONDUCTIVITY, $T_f = 45°F$

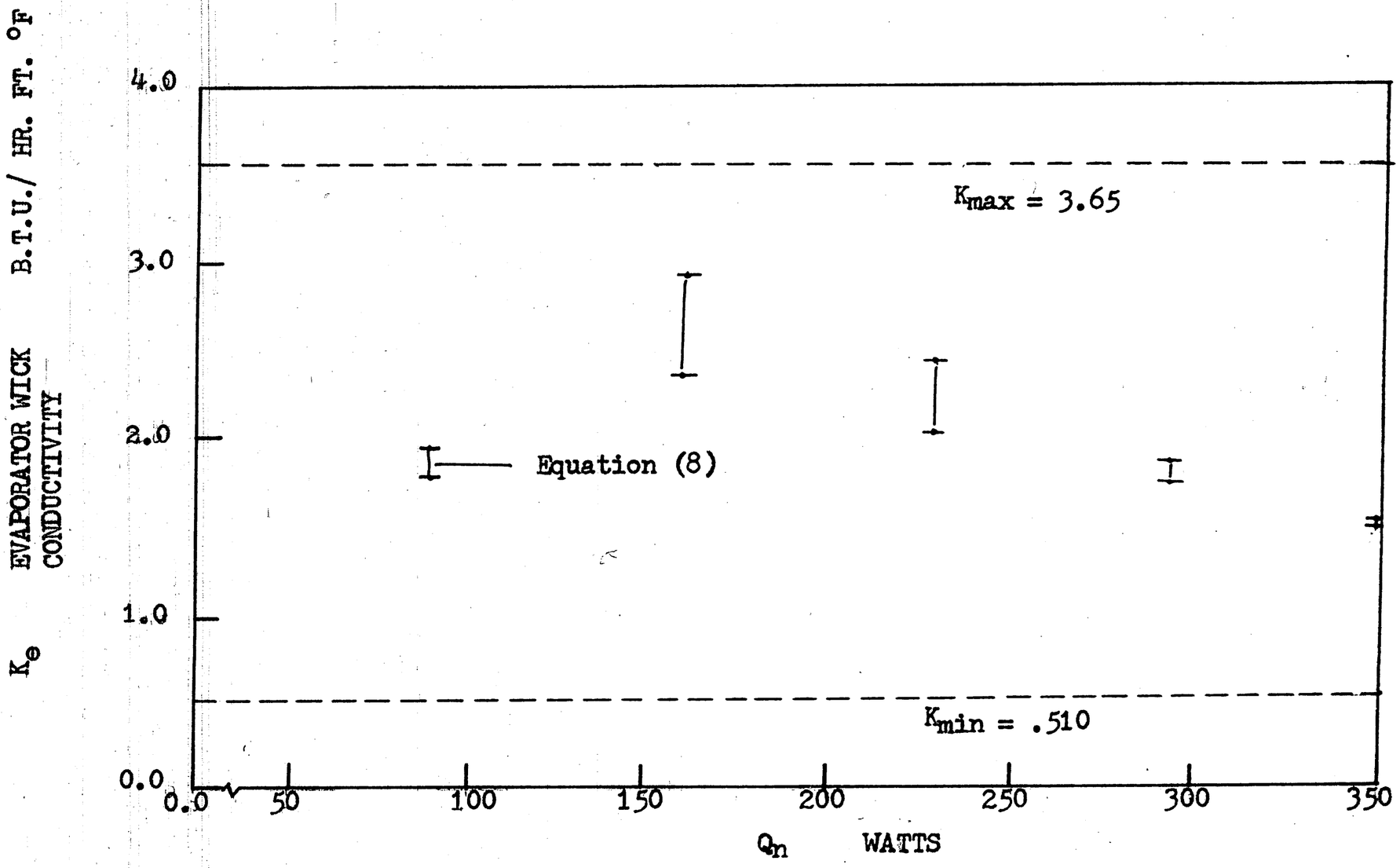

FIGURE 19. EVAPORATOR WICK CONDUCTIVITY, $T_f = 70°F$

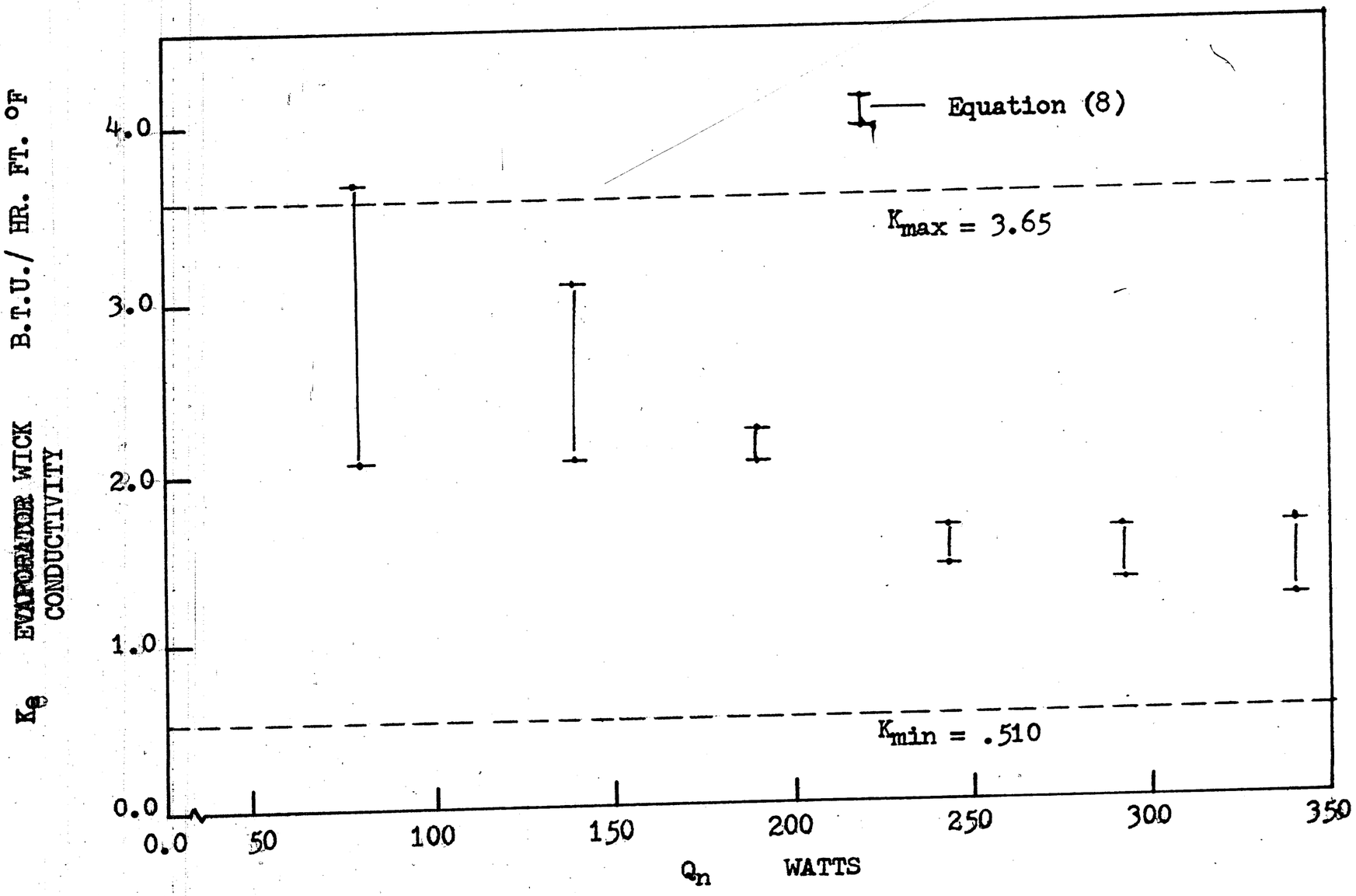

FIGURE 20. EVAPORATOR WICK CONDUCTIVITY, T_f = 90 °F

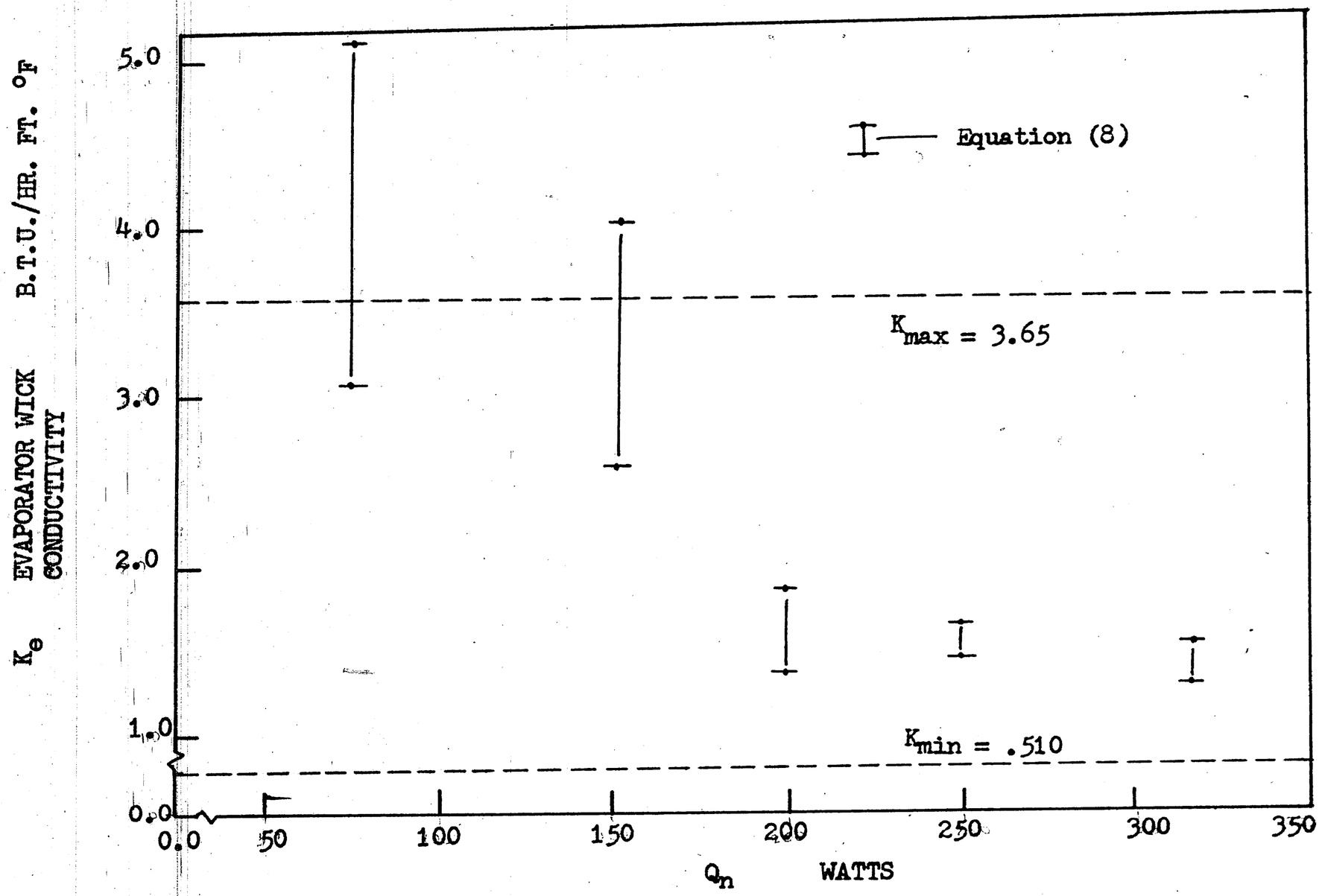

FIGURE 21. EVAPORATOR WICK CONDUCTIVITY, T_f = 112 °F

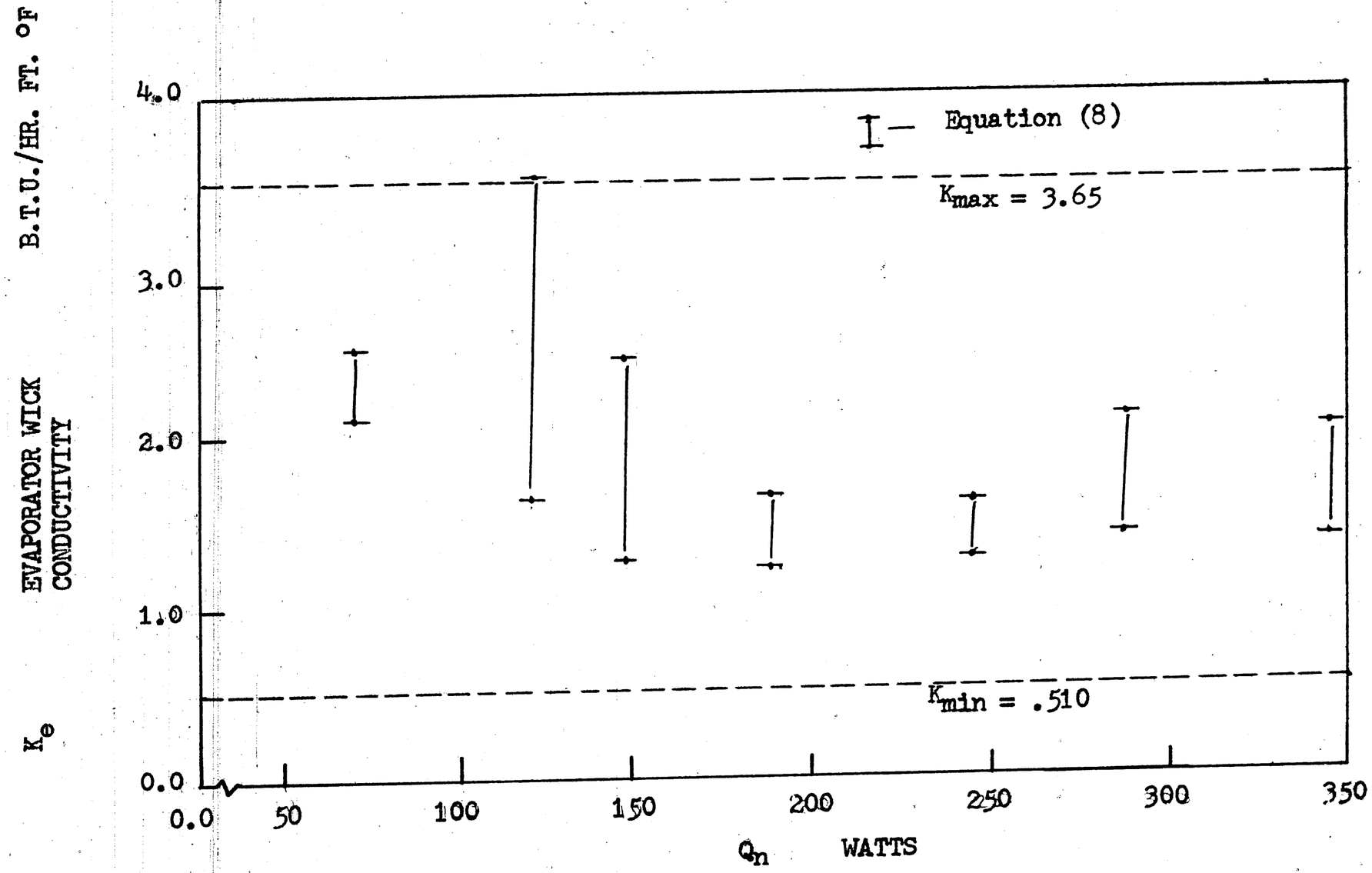

FIGURE 22. EVAPORATOR WICK CONDUCTIVITY, T_f = 140 °F

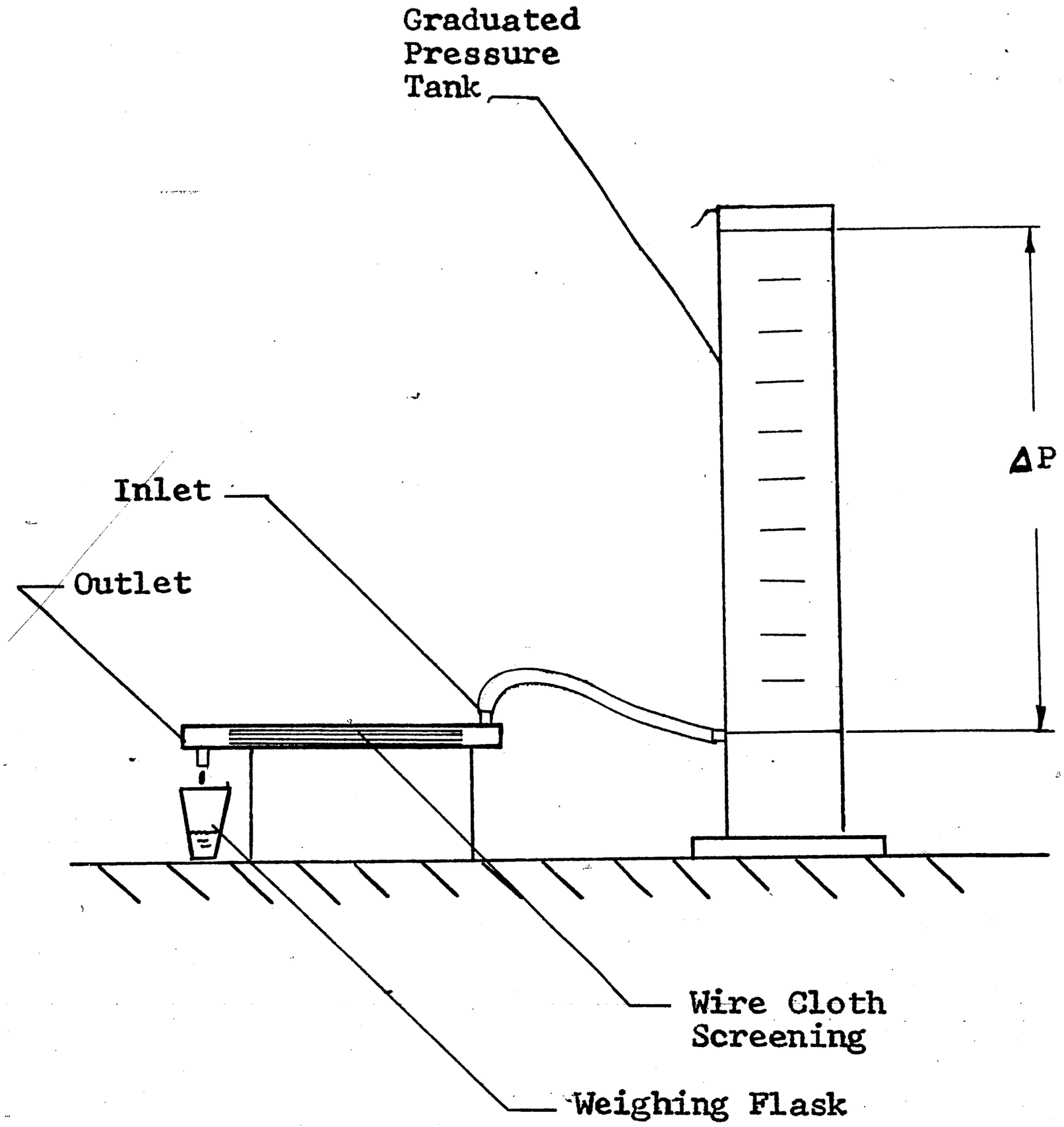

FIGURE 23. PERMEABILITY EXPERIMENTAL APPARATUS

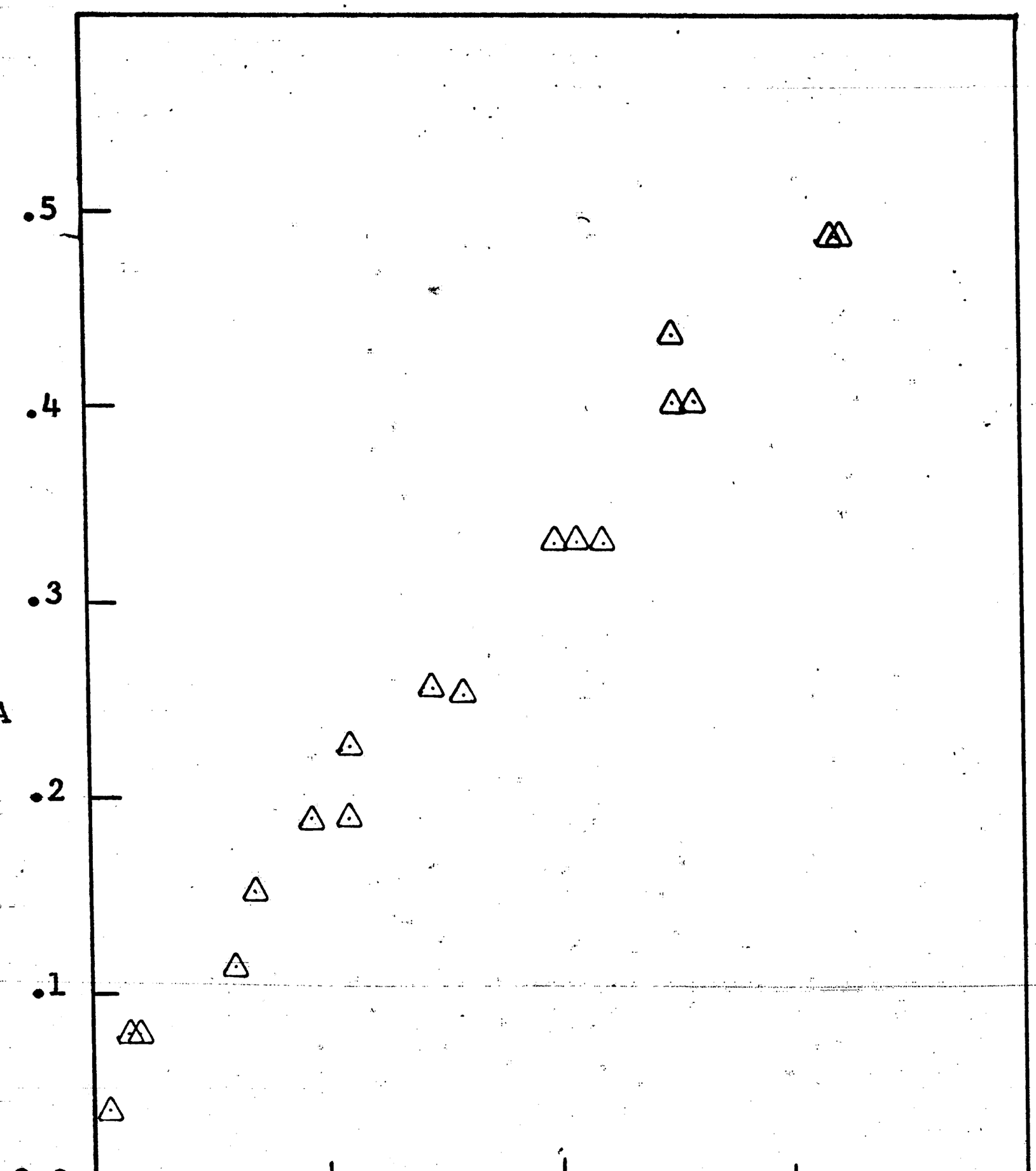

FIGURE 24. PERMEABILITY EXPERIMENT RESULTS

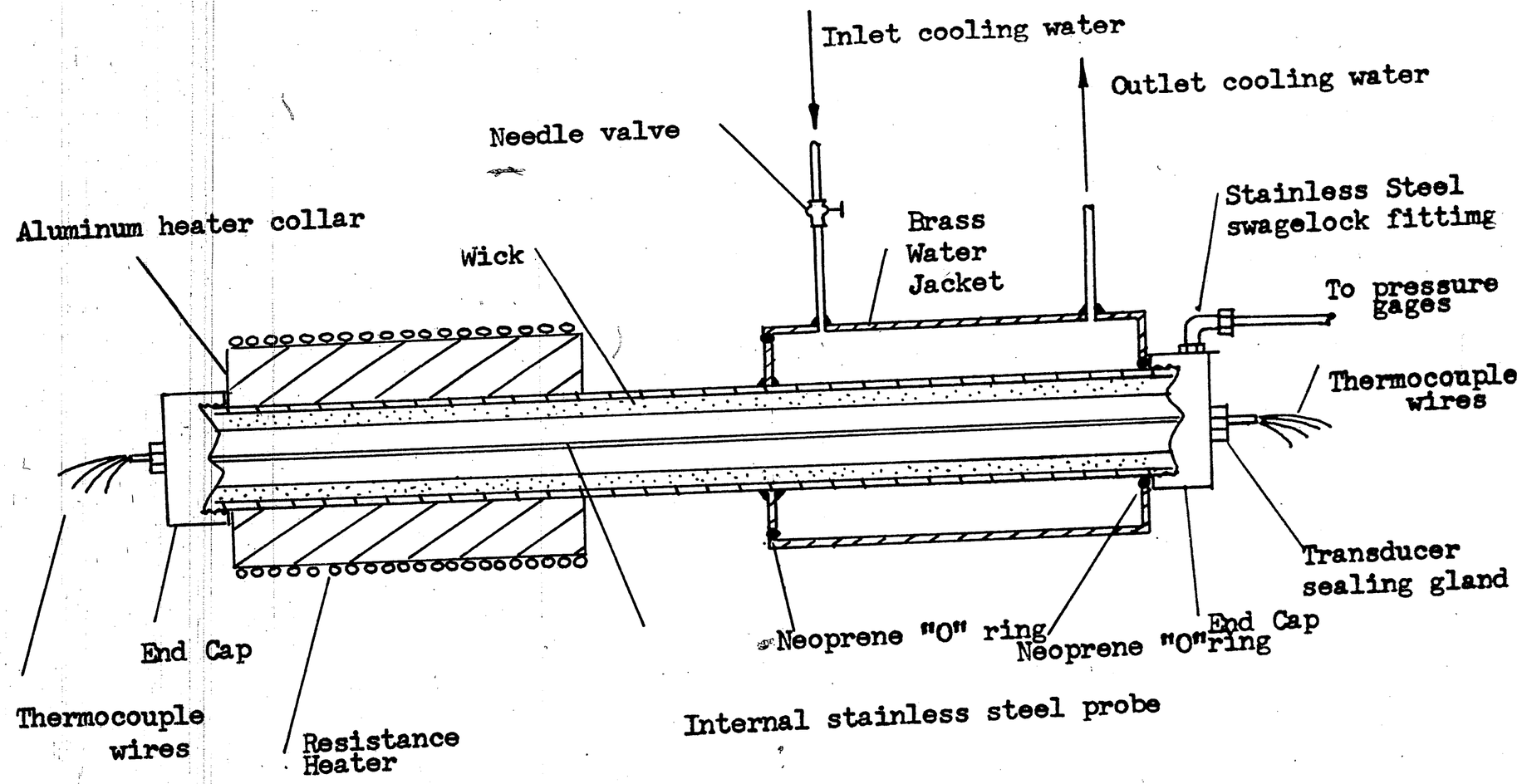

Figure 25. Schematic of Heat Pipe, Heat Source, and Heat Sink

LIST OF REFERENCES

1. Patent Disclosure No. 48148, D. C. Thompson, February 10, 1960.

2. " Structures of Very High Thermal Conductance", G. M. Grover, T. P. Cotter, and G. F. Erickson, Journal of Applied Physics, 35, 1964, P 1990.

3. " Theory Of Heat Pipes", T. P. Cotter, LA-3246-MS, Los Alamos Scientific Laboratory, 1965.

4. " Heat Pipe Analysis", G. H. Parker and J. P. Hanson, Intersociety of Energy Conversion Conference, 1967.

5. " Heat Pipe Capability Experiments", J. E. Kemme, Thermionic Conversion Specialist Conference, Nov. 1966.

6. " Theoretical Investigation of Heat Pipes Operating at Low Vapor Pressures", E. K. Levy, ASME Journal Of Engineering For Industry, Vol. 90, Nov. 1968, P 547.

7. " The Heat Pipe", K. T. Feldman, Jr., G. H. Whiting, Mechanical Engineering, Feb. 1967.

8. Principles of Heat Transfer, 2nd Ed., F. Kreith, International Textbook Co., Scranton, Pa., 1966.

9. " Thermal Conductivity of Hetrogeneous Materials", Chemical Engineering Progress, Vol. 57. No. 7, P 53-59, July 1961.

10. Conduction Heat Transfer, T. J. Schneider, Addison-Wesley Publishing Co., Reading Mass., 1955.

11. "Engineering Study of Vapor Cycle Cooling Components For Space Vehicles, R. Grinwala, T. A. Blatt, R. W. Bilgor, Technical Document Report No. ASD-TDR- 63-582, Sept. 1963, AirfForce Flight Dynamics Laboratory, Air Force System Command, Wright-Patterson Air Force BAse, Ohio, P 120-148

12. " Vapor Chamber Fin Studies", H.R. Kunz, L. S. Langston, B. H. Hilton, S.S. Wyde, and G. H. Nashick, NASA Report CR-812, Pratt and Whitney Aircraft, June 1967.

VITA

Nathan Kalowski was born in Lodz, Poland on May 13, 1945. He is the son of Mr. and Mrs. Leonard Kalowski of 19 Summit Avenue, Providence, Rhode Island, and has one brother, Jeffrey.

He immigrated to the United States in 1951 and attended Providence Hebrew Day School, Roger Williams Junior High School, and Classical High School from which he graduated in June, 1963.

On June 11, 1967 he received a B.S. in Mechanical Engineering from the University of Rhode Island. While at the University of Rhode Island he was a member of the varsity tennis team and crew team. He was a member of the A.S.M.E. and its Secretary, and won the A.S.M.E. senior outstanding member award. He was also a member of Tau Beta Pi and Phi Sigma Delta social fraternity.

From September, 1967 to February, 1969, Mr. Kalowski was a graduate teaching assistant at Lehigh University where he obtained his M.S. in Mechanical Engineering.